

FINAL PUBLISHABLE JRP REPORT

JRP-Contract number	IND01	
JRP short name	HITEMS	
JRP full title	High temperature metrology for industrial applications (>1000 °C)	
Version numbers of latest contracted Annex Ia and Annex Ib against which the assessment will be made	Annex Ia:	V1.4
	Annex Ib:	V1.0
Period covered (dates)	From	1 September 2011 to 31 August 2014
JRP-Coordinator		
Name, title, organisation	Graham Machin, Prof, NPL, United Kingdom	
Tel:	+44 (0)208 943 6742	
Email:	graham.machin@npl.co.uk	
JRP website address	http://projects.npl.co.uk/hitems/	
Other JRP-Partners	CEM, Spain CMI, Czech Republic CNAM, France INRIM, Italy LNE, France PTB, Germany SMU, Slovakia UME, Turkey VSL, The Netherlands CEA, France E+H, Germany GDF, France MSS, United Kingdom	
REG1-Researcher (associated Home Organisation)	Marco Seifert FhG, Germany	Start Date: 1 December 2011 Duration: 24 months
REG2-Researcher (associated Home Organisation)	Matthias Rydzek ZAE, Germany	Start Date: 1 May 2012 Duration: 24 months
RMG1-Researcher (associated Home Organisation)	Peter Pavlasek SMU	Start Date: 1 Oct 2012 Duration: 6 months
RMG2-Researcher (associated Home Organisation)	Lenka Knazovicka CMI	Start Date: 1 Nov 2013 Duration: 3 months

Report Status: PU Public

TABLE OF CONTENTS

1	<i>Executive Summary</i>	3
2	<i>Project context, rationale and objectives</i>	4
3	<i>Research results</i>	6
3.1	Rigorous, traceable techniques to enable lifetime and stability evaluation of contact temperature sensors above 1000 °C	6
3.1.1	Procedure for lifetime testing.....	6
3.1.2	Procedure for drift testing.....	6
3.1.2.1	Drift: short term.....	7
3.1.2.2	Drift: long term.....	7
3.1.2.3	Tests.....	7
3.2	Self-validating contact temperature sensors for use from 1000 °C to above 2000 °C	11
3.3	A methodology for the rigorous determination of ‘reference functions’ for non-standard thermocouple types	19
3.3.1	Description of the facilities developed for this objective.....	20
3.3.1.1	CEM facilities.....	20
3.3.1.2	LNE-CNAM facilities.....	21
3.3.1.3	NPL facilities.....	21
3.3.1.4	SMU facilities.....	22
3.3.1.5	Determination of the Pt-40%Rh versus Pt-20%Rh thermocouple reference function.....	22
3.3.1.6	Ramifications of the findings (progress beyond the state of the art).....	25
3.3.1.6.1	Melting temperature of palladium.....	25
3.3.1.6.2	Melting temperature of platinum.....	25
3.3.1.6.3	Summary.....	26
3.4	Traceable and accurate radiation measurement techniques for in situ surface high temperature measurements above 1000 °C	27
3.4.1	UV-multiwavelength techniques for simultaneous temperature and emissivity measurements.....	27
3.4.2	Determining the size-of-source effect using scanning method.....	28
3.4.3	Best measurement practice for using gold-cup radiation thermometers on curved and sloped surfaces.....	29
3.4.4	Absolute thermovisual characterisation of thermal imager.....	30
3.4.5	Improvement and validation of active two-colour laser-based radiation thermometer.....	31
3.4.6	Temperature-independent emissivity measurement using the virtual source technique.....	32
3.5	In-situ validation methods for non-contact thermometry to above 2500 °C	34
3.5.1	Development and characterisation of the cells.....	34
3.5.1.1	Graphite cells for inert atmospheres.....	35
3.5.1.2	Alumina cells for oxidising atmospheres.....	36
3.5.2	In-situ test results.....	37
3.5.2.1	Measurements at CEA.....	37
3.5.2.2	Measurements at GDF-Suez.....	38
3.5.3	Conclusions.....	39
3.6	In-situ traceable temperature measurements for exotic thermal processing methods	39
4	<i>Actual and potential impact</i>	41
5	<i>Website address</i>	45
6	<i>List of publications (published on date of submission)</i>	45

1 Executive Summary

Introduction

This project developed techniques for industrial users to more accurately measure temperatures above 1000 °C. This research advanced the state of the art in temperature measurement by developing methods to compensate for sources of uncertainty in radiation thermometry, to re-calibrate contact thermometers *in situ*, and to develop and characterise the performance of non-standard contact thermometers. These new measurement techniques will be used across a range of industries to better control high-temperature processes, improving energy efficiency, ensuring uniform product quality, and minimising emissions.

The Problem

The accurate measurement of high-temperatures is vital to a wide range of EU industries. Using the right temperature ensures that (i) processes are energy-efficient, minimising production costs and greenhouse gas emissions; (ii) that components produced at high-temperatures consistently meet quality standards (e.g. are not damaged through overheating), and (iii) that process temperatures do not exceed safety standards (for instance in the nuclear industry). Ultimately, the more accurate measurement of temperatures will support improved EU industrial competitiveness whilst minimising its environmental impact.

Although high-temperature processes are used routinely in industries such as aerospace/space (~1300-3000 °C); nuclear (~1800->2500 °C); refractory metals production (>2500 °C); silicon carbide, carbon and carbon composites production (>2800 °C); iron, steel, glass and ceramics production (2000 °C); measuring temperatures above 1000 °C is difficult. Improved measurement techniques are required that accurately and consistently measure temperatures above 1000 °C, and do so *in-situ* (during the process), to ensure that high-temperature processes can be controlled effectively.

The Solution

The HiTeMS project developed a suite of methods and techniques to measure more effectively high temperatures in hostile environments.

Outstanding issues surrounding contact thermometry were addressed by developing a standard experimental process and NMI facilities traceable to the International Temperature Scale of 1990 (ITS-90) to test the lifetime and drift of base metal thermocouples and the drift of noble metal thermocouples. Sensor self-validation methods to above 2000 °C, which are capable of in-situ use, were developed. A distributed capability for the rapid, accurate determination of reference functions of novel thermocouples to 2000 °C was assembled.

The problems associated with improving the reliability of industrial non-contact thermometry were investigated through a) developing an ultraviolet multiwavelength pyrometer b) putting gold cup pyrometry onto a traceable footing and c) validation of active two colour pyrometry. The uncertainties associated with gold cup pyrometry, which is widely used in industry, are now much better understood. In-process methods for the reliable determination of pyrometer drift and corrections for varying window transmission were developed and demonstrated.

Impact

The HiTeMS project achieved significant impact during the lifetime of the project, with further substantial ongoing impact expected for a broad range of industries, with highlights including:

The EURAMET guide for lifetime drift testing of thermocouples is currently being used by a number of contact thermometer manufacturers to test their products. The performance details they produce will help industrial users to select the most appropriate thermocouples for their processes.

During the production of the guide, a number of manufacturers provided sample thermocouples for testing. Feedback on their performance has enabled the manufacturers to better understand the limitations of their sensors, allowing them to improve their performance.

The approaches we demonstrated for re-calibrating thermocouples *in situ* will be further developed in EMPIR project EMPRESS. Self-calibrating thermocouples suitable for use in industrial settings will be constructed and trailed by 2018.

The facility for determining reference functions for novel thermocouples has allowed us to investigate new thermocouple types, and will be used by the EMPIR EMPRESS project to develop high-temperature, low/no drift thermocouples. These thermocouples will be trialled in industry before the end of the project in 2018. An industrial partner is keen to exploit this development.

The facility for investigating gold cup pyrometer performance is now available for industrial users to estimate and address the sources of temperature uncertainty in industrial processes.

The use of high-temperature fixed point blackbodies to determine window transmission has the potential to significantly improve temperature measurement for essential nuclear safety testing, leading to the safer use of nuclear reactors for power generation.

The demonstration of accurate *in-situ* temperature measurement during laser hardening has the potential to dramatically improve process control in this growing industry.

2 Project context, rationale and objectives

The overall purpose of the project was to improve high temperature thermometry above 1000 °C up to at least 2500 °C. This is important for a number of reasons; at a high level to improve industrial process efficiency both in terms of output and also in terms of energy use, and to reduce carbon emissions. At a technical level the project sought to develop new methods, capabilities and approaches to high temperature measurement addressing unsolved measurement challenges in industry and improving measurement reliability and, in particular, aiming to introduce traceability to the International Temperature Scale of 1990 (ITS-90) directly within the industrial process. Essentially industrialists require better knowledge of the performance of their temperature sensing methods. Such knowledge informs decisions about process control and that in turn determines product quality, process efficiency both in terms of output and energy use. Optimising energy use in turn ensures that carbon emissions are as low as possible commensurate with these other objectives.

Industry use two broad approaches to measure high-temperatures: **contact thermometry** that uses temperature sensors, such as thermocouples or resistance thermometers, where temperature measurement is performed using sensors directly in contact with the industrial process, and **non-contact thermometry** that measures temperature at a distance by analysing the thermal radiation an object emits at different temperatures. Both approaches present challenges at high temperatures.

For contact thermometry, the performance of thermocouples changes considerably over time (mainly through undetected but significant drifts) and the hostile environments of high-temperature processes restricts access for servicing and re-calibration. Novel thermocouples based on non-standard materials could be better suited to high temperature applications, but their use is limited as their performance is not fully understood. The technical capability for their standardisation, (and thus access to the new sensors) was developed in this project.

Non-contact-thermometry offers many advantages over contact thermometry in high temperature environments and while it is increasingly used in a range of industries, it suffers from a number of sources of measurement uncertainty such as unknown emissivity (different materials emit light differently) and high levels of background thermal radiation.

The HiTeMS project aimed to improve the reliability of temperature measurement at high temperatures and to address specific problems associated with the hostile environment for both contact and non-contact thermometry. Its objectives were as follows:

Contact thermometry:

1. Rigorous, traceable techniques to enable lifetime testing and stability evaluation of contact temperature sensors above 1000 °C. There was no agreed method of drift and lifetime testing of thermocouples. The project developed a lifetime and drift testing capability, including the development of an authoritative EURAMET guide for performing such tests.
2. Self-validating contact temperature sensors for use from 1000 °C to above 2000 °C demonstrated. Contact thermometry sensors drift, sometimes very rapidly, when exposed to high temperatures. The project will improve in-process temperature measurement by an uncertainty factor of 10 or more through developing novel self-validating thermocouples.
3. A methodology for the rigorous determination of 'reference functions' for non-standard thermocouple types. Thermocouples suitable for high-temperature processes and harsh environments are currently not used as their reference functions have not been defined. The project will develop tools in the EU national

measurement institute (NMI) community to rapidly define the reference functions of non-standard thermocouples (and potentially other temperature sensors).

Non-contact thermometry:

4. Traceable and accurate radiation measurement techniques for *in-situ* surface high temperature measurements above 1000 °C. Temperature measurement by radiation thermometry is a rapidly growing measurement method in a broad spectrum of industries. The project will develop solutions to the significant accuracy limiting factors; unknown emissivity, background radiation and size of source effect.
5. *In-situ* validation methods for non-contact thermometry to 2500 °C, including demonstrating novel drift correcting techniques. At high-temperatures, radiation thermometry accuracy is limited by window contamination (which also requires scheduled stoppage for cleaning or replacement), and shifts in calibration. The project will demonstrate *in-situ*, quasi-real time correction of these two intractable problems by incorporating known, stable high-temperature references within the industrial process.
6. A demonstration of *in-situ* traceable temperature measurements for exotic thermal processing methods such as laser hardening. The project will demonstrate traceable and accurate non-contact thermometry in a challenging industrial setting, where it has not been achieved before. Laser hardening has been selected as it is an industrial technique used widely throughout the EU.

3 Research results

3.1 *Rigorous, traceable techniques to enable lifetime and stability evaluation of contact temperature sensors above 1000 °C*

This objective aimed to put, for the first time, drift characterisation of base and noble metal thermocouples on a sound metrological footing within NMIs. It is vital to understand the drift characteristics of such sensors as they are so widely used in industry and any improvements that might be proposed can be precisely benchmarked against such facilities.

This research stream aimed to establish a rigorous means of determining the lifetime characteristics of base metal thermocouples and the drift characteristics of base metal and noble metal thermocouples, firmly grounded in traceability to the SI (i.e. to the ITS-90). The work initially established the lifetime and drift testing capability in the laboratory. This included validation of that capability with thermocouples supplied by sensor manufacturers. The results from testing different types of thermocouple facilitate better understanding of the processes (e.g. chemical, physical) causing the drifts.

Transfer of the results of these investigations to industrial sectors is important. In addition the whole EU NMI temperature metrology community will benefit from the outcome of this study through the development of a EURAMET guide on the lifetime and drift assessment of thermocouples.

The first step in this investigation was the evaluation and improvement of the current lifetime and drift assessment methods for base metal and noble metal thermocouples used in high temperature applications. Current methods are rather ad-hoc, often differing between sensor producer and user leading to misunderstanding. That is why, the standardised apparatus and procedure for evaluating the lifetime performance of thermocouples suited for temperatures up to 1800 °C were prepared at different NMIs.

Next the protocol for testing of the thermocouples was prepared. It can be divided to the two sections:

3.1.1 *Procedure for lifetime testing*

For determining establishing the lifetime it is recommended to use new, untreated and uncalibrated thermocouples. The following procedure is recommended for base metal thermocouples:

1. Prior to starting the test the thermocouples must not be subject to any heat treatment, e.g. calibration or annealing.
2. Use a good quality temperature standard for determining the furnace temperature.
3. Test the thermocouples at the desired temperature. For example, the testing temperature may be determined on the basis of the supplier's specification of the maximum allowable temperature for short term use with addition of 5 %.
4. Connect all thermocouples to the multimeter (use only a switchbox with known properties) or A-to-D converter.
5. Continuous measurement of the thermocouples (with automatic or manual data logging), the furnace temperature is checked with the reference thermometer periodically (e.g. once per week).
6. The test, for a given thermocouple, should be terminated if
 - a. There is no output from the thermocouple, or
 - b. The drift of deviation of the tested thermocouple from standard EN IEC 60584-1 exceeds the desired tolerance.

The lifetime of the thermocouple calibration is determined as the time elapsed between the start of the test (Step 3) and its termination (Step 6).

3.1.2 *Procedure for drift testing*

- Procedure for testing short term drift
- Procedure for testing long term drift

It is expected that these tests will be performed at different temperatures.

3.1.2.1 Drift: short term

This test should be applied to a calibrated and properly annealed thermocouple. Recommended procedure for determining thermocouple short term drift/stability is as follows:

1. Calibration of the test thermocouple at the maximum temperature of intended use and a homogeneity check performance.
2. Testing of the thermocouples at the desired temperature.
3. The duration of the test is 8 hours maximum
4. Calibration of the thermocouple at the maximum temperature of intended use.
5. Repeat steps 3 to 4 three times.

The calibration drift is determined as the output change (or its temperature equivalent) between the first calibration and the final calibration.

3.1.2.2 Drift: long term

This test should be applied to a calibrated and properly annealed thermocouple. Recommended procedure for determining thermocouple long term drift/stability is as follows:

1. Calibration of the test thermocouple at the maximum temperature of intended use and a homogeneity check performance
2. Testing of the thermocouples at the desired temperature.
3. The duration of the test is 4 months at minimum.
4. Calibration of the tested thermocouple at the maximum temperature of intended use every week during the first month and every 2 weeks for the following months.
5. The test(s) are finished if
 - a) The agreed final time is reached, or
 - b) There is no output from the thermocouple, or
 - c) The deviation of the tested thermocouple from standard EN IEC 60584-1 exceeds 3 times the desired tolerance.

The calibration drift is determined as the change in EMF (or its temperature equivalent) from the first measurement to the termination

3.1.2.3 Tests

For the tests, selected batch of noble and base metal thermocouples were prepared and sent to the NMIs – see Table 1

Table 1 Selected thermocouples for lifetime and drift tests

Producer	Life time 1300 °C	Drift long term 1000 °C a 1100 °C	drift short term 1100 °C a 1300 °C	drift long term 1000 °C a 1720 °C	drift short term 1600 °C 1820 °C
Omega	5 × 1 mm	3 × 1 mm	2 × 1 mm		
	5 × 3 mm	3 × 3 mm	2 × 3 mm		
	5 × 6 mm	3 × 6 mm	2 × 6 mm		
	4 × 1 mm	2 × 1 mm	2 × 1 mm		
CCPI	4 × 3 mm	2 × 3 mm	2 × 3 mm		
	4 × 6 mm	2 × 6 mm	2 × 6 mm		
	4 × 1 mm	3 × 1 mm	2 × 1 mm	2 × type B	1 × type B
Meggit	4 × 3 mm	3 × 3 mm	2 × 3 mm	2 × type R	1 × type R
	4 × 6 mm	3 × 6 mm	2 × 6 mm	2 × type S	1 × type S
	2 × 1,5 mm				
	2 × 2 mm	1 × 1,5 mm	1 × 1,5 mm		
	2 × 3 mm	1 × 3 mm	1 × 3 mm		
	2 × 4 mm	1 × 4 mm	1 × 4 mm		
Zpa Nová Paka	2 × 6 mm	1 × 6 mm	1 × 6 mm		

CMI (CZ), SMU (SL), LNE-Cnam (F) and UME (TU) provided tests according to the procedure described above. Some results are given in the following pictures.

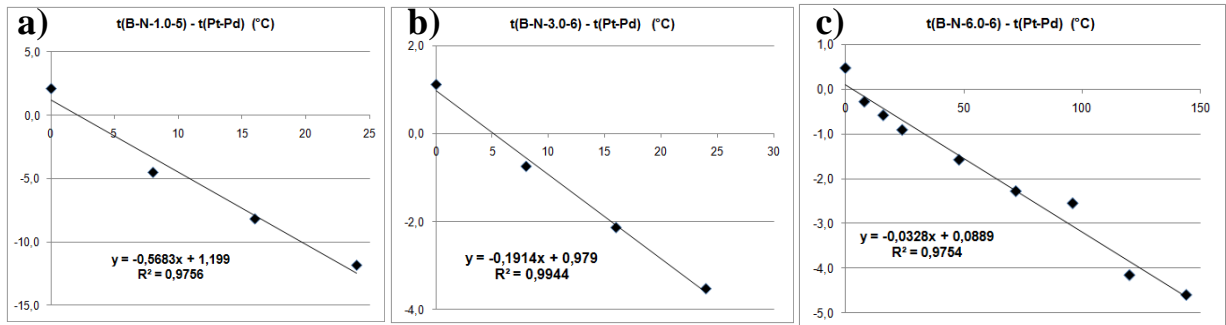


Figure 1 Typical drift measured with type N thermocouples during short-term drift tests at 1300 °C ; a) 3 mm diameter ; b) 3 mm diameter ; c) 6 mm diameter

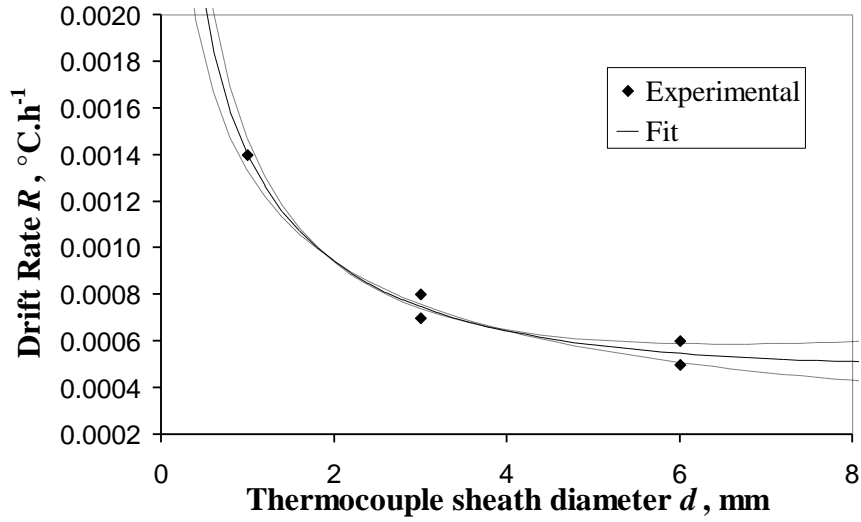


Figure 2 Influence of the diameter on the drift rate of a batch of type K thermocouples exposed to a temperature of 1000 °C during 800 h. Tolerances of the model are shown by the dashed lines.

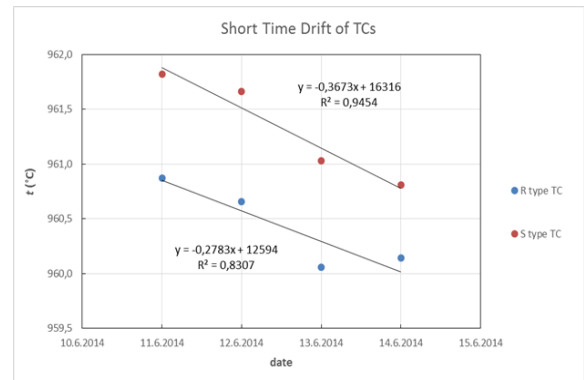
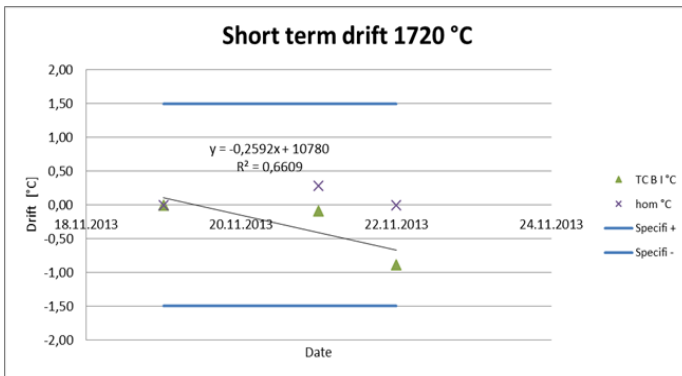


Figure 3 Short term drift of B, S and R type thermocouples

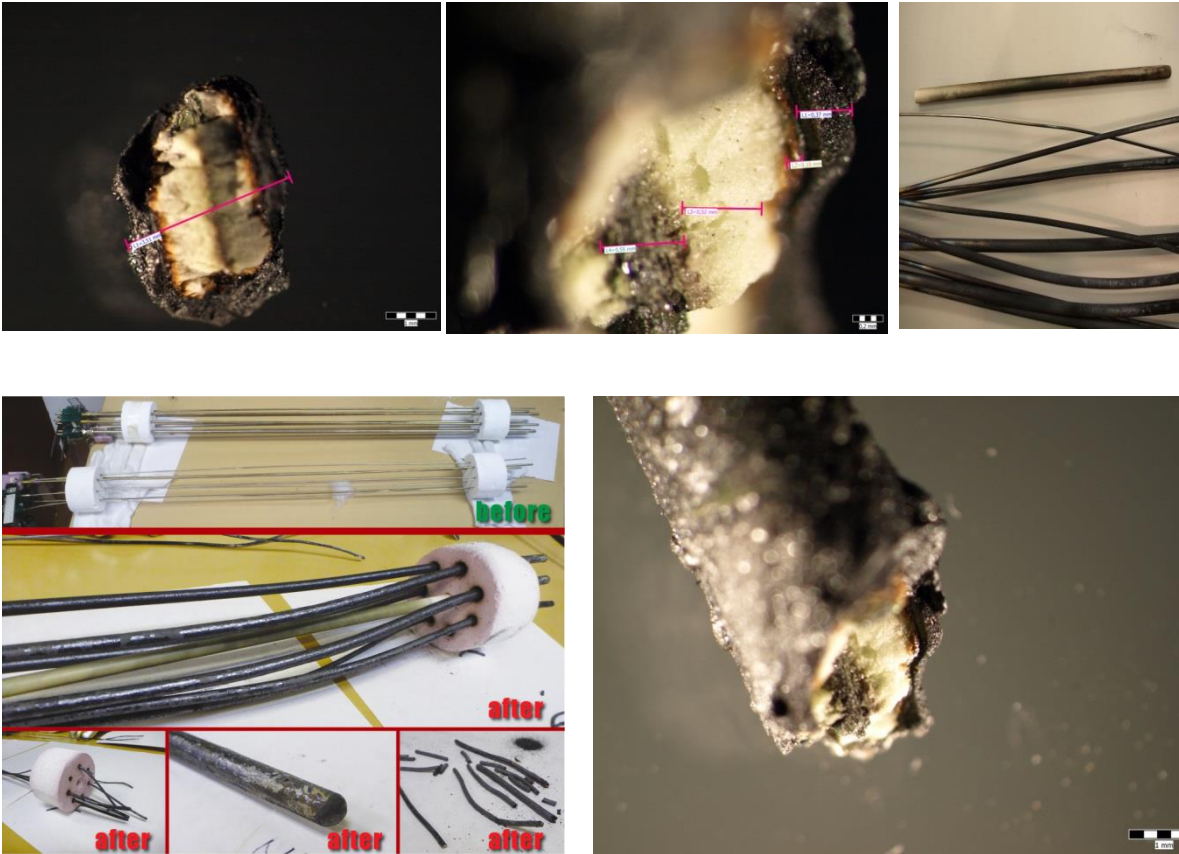


Figure 4 Pictures of base metal thermocouples after life time tests.

The investigation of drift dependence on the thermocouple diameter was also done. The example of the result is shown on Figure 5.

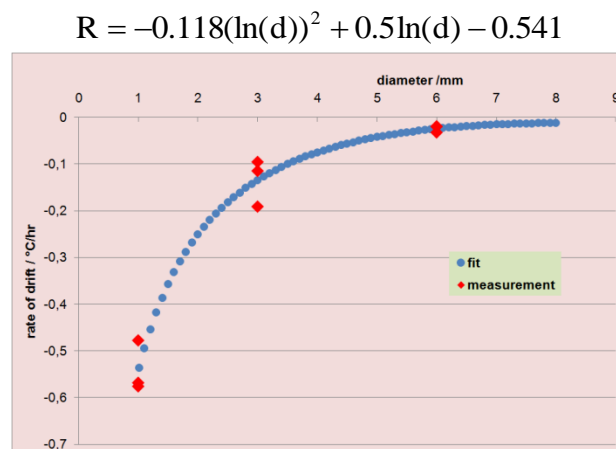


Figure 5 Rate of drift at 960 °C (N type)

The objective of this body of work was to develop rigorous traceable techniques to enable lifetime testing and stability evaluation of temperature sensors at 1000 °C and above.

Previously no general methodology was available for determination of the lifetime characteristics of base metal thermocouples and the drift characteristics of base metal and noble metal thermocouples. Industrial organisations and NMI would perform these tests based on an internal procedure which were not validated nor were intercomparisons between organisations viable.

Extensive testing of a number of different thermocouples was performed by a number of different partner organisations. These tests followed testing procedures developed from a survey of existing methods used by different organisations. From the results a Good Practice Guide was written and presented to industrial organisations for industrial tests. The results were positive and the GPG has become a EURAMET GPG, available to the public through the EURAMET website. Furthermore the methodologies have been adopted in the industrial organisations where testing was performed.

3.2 Self-validating contact temperature sensors for use from 1000 °C to above 2000 °C

This objective sought to address the need for self-validation and *in-situ* validation methods of contact thermometry between 1000 °C and above 2000 °C. This is extremely important for industrial applications which often relied on very unsatisfactory temperature sensors, for instance W/Re thermocouples. Improvements in sensing methods, especially *in-situ* validation, may bring about a step change improvement in the practice of thermometry and hence industrial process control.

The two self-validation concepts investigated are based on the use of miniature fixed points with defined and stable melting temperatures of pure metals or metal-carbon (Me-C) eutectics which are combined directly with commonly used thermocouples to detect their drift effects. The second self-validation concept is based on the simultaneous use of noise thermometry as (primary) method to measure temperatures without drift effects to validate for instance the thermoelectric stability of thermocouples as parts of a combined thermocouple-noise temperature sensor. A general overview about noise thermometry can be found in [3.1], details of the used noise thermometer are described in [3.2].

Firstly, material compatibility studies were started to identify suitable candidate materials for miniature high-temperature fixed points (HTFPs) and insulators which can be used at high temperatures around 2000 °C in inert atmospheres or vacuum conditions for use with conventional mineral insulated metal sheathed (MIMS) W/Re thermocouples. The main challenge was to find suitable fixed-point materials and a crucible material that is compatible to the fixed-point material and to the components of the MIMS thermocouples. Different material combinations were investigated up to 2300 °C. Two high-temperature fixed-point cells made of pure carbon and filled with Pt-C (1738 °C) and Ru-C (1953 °C) were constructed for use with MIMS format thermocouples (Figure 6). Available sheath materials for MIMS thermocouples, molybdenum and tantalum, were tested in direct contact with carbon which was used as crucible material. Both metals showed reaction resulting in the forming of the corresponding carbides but in a less extent for tantalum, which was therefore chosen as sheath material of the MIMS W/Re thermocouples. Nevertheless, the diffusion of carbon into the tantalum should be suppressed by using a suitable protection material which doesn't suffer from reactions both with tantalum and carbon. Among four tested ceramics, hafnia and yttria-stabilised zirconia remained noticeably more robust after the 2000 °C and 2300 °C tests when exposed to carbon than the other two, boron nitride and silicon carbide. Both of the former may be suitable for use as protection materials, with the correct design geometry to maximise the suppression of reactions between carbon and tantalum [3.3].

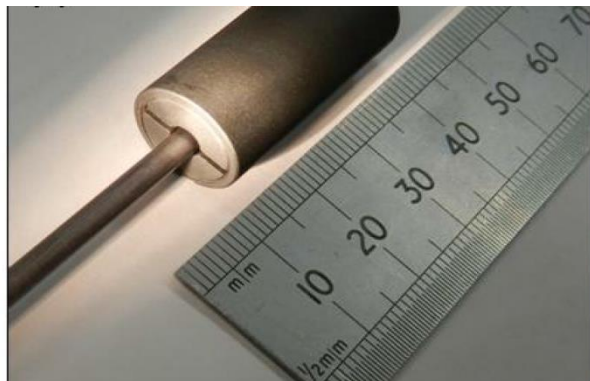


Figure 6 High-temperature miniature fixed point filled with a Me-C eutectic and usable with MIMS thermocouples

To investigate the long-term stability of the high-temperature fixed-point cells Pt-C and Ru-C they were annealed for 2225 h at $T \approx 1727 \text{ }^\circ\text{C}$ (about 10 K below the melting temperature T_S) by using three W-Re (type C) thermocouples (Pt-C) and for 1600 h at $T \approx 1943 \text{ }^\circ\text{C}$ (about 10 K below T_S) by using two type C thermocouples (Ru-C). Repeated melting and freezing cycles (Pt-C: 33 cycles, Ru-C: 25 cycles) were realised during this heat treatment. The measured emfs of the melts are shown in Figure 7 **Error! Reference source not found.** for the Pt-C miniature fixed point and in Figure 8 **Error! Reference source not found.** for the Ru-C fixed point. Before and after finishing the heat treatment the melting temperatures of the both miniature fixed points were measured by using a radiation thermometer. The melting temperatures agreed within 0.2 K by using the Pt-C cell and within 0.4 K by using the Ru-C cell. The measurement uncertainty of the radiation temperature measurement was about 1 K. Therefore, the melting temperatures of both miniature fixed point cells remain stable within some tenth of a Kelvin and the drifts observable in the Figure 7 and Figure 8 are caused by thermoelectric instabilities of the type C thermocouples used. This clearly demonstrates the ability of the investigated Pt-C and Ru-C cells to detect drift effects of thermocouples in the order of a few tenth of a Kelvin.

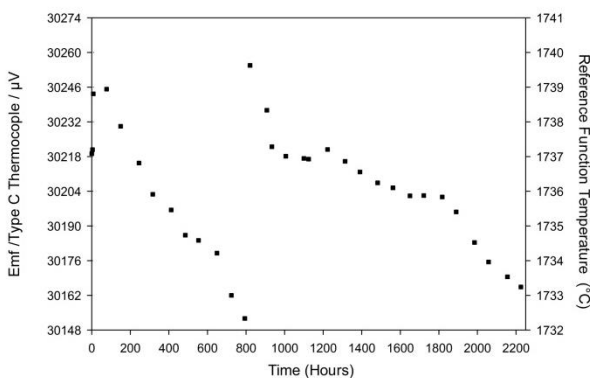


Figure 7 Emfs of the melts by using the Pt-C miniature fixed point with type C thermocouples

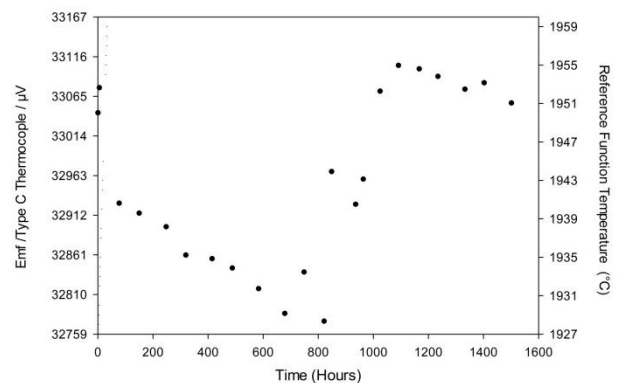


Figure 8 Emfs of the melts by using the Ru-C miniature fixed point with type C thermocouples

Four different designs of self-validating structures usable in oxidising atmospheres up to 1800 °C including miniature fixed-point cells have been constructed and investigated. The miniature cells were made of Alumina 99.7% and pure metals of platinum or palladium were used as fixed-point materials. Figure 9 shows the general designs of the miniature fixed points [3.4]. Innovative self-validation methods of high temperature thermocouples developed involved methods of using thick wires in multibore insulators as fixed-point materials [3.5], as presented in Figure 10.

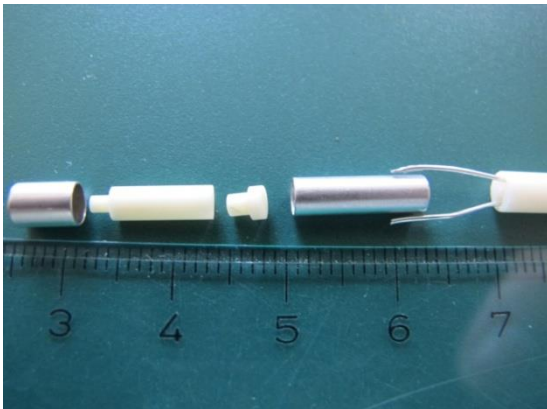


Figure 9 Miniature fixed point (design A) welded between the thermoelements (left) and miniature fixed points (design B) surrounding the measurement junctions of thermocouples (right)

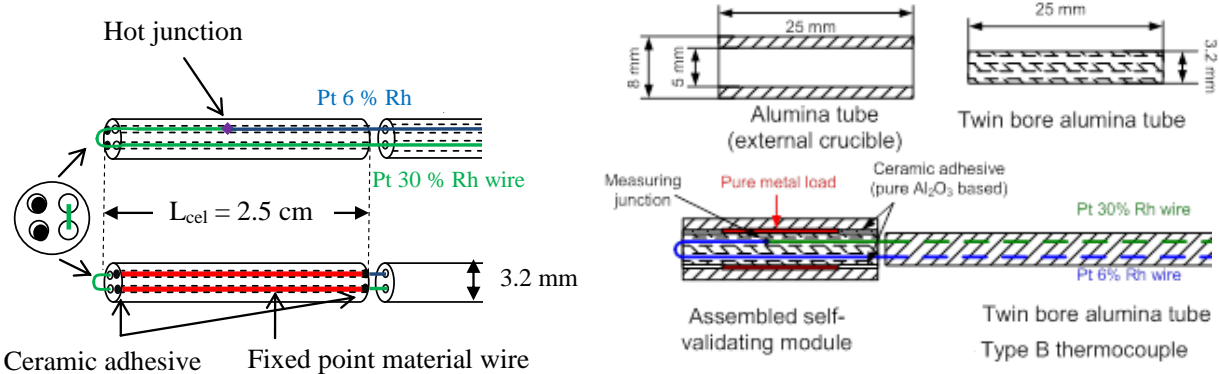


Figure 10 Integrated self-validating pulled-wire (PW) module (left) and embedded self-validating rolled-wire (RW) module (right)

A typical melting curve of palladium ($T_s = 1553.4\text{ °C}$ in air) by using the type B thermocouple SV-B-Pd-01-12 with the integrated fixed-point crucible Pd-01-12 (design A) against the emf of the furnace control thermocouple is shown in Figure 11. The melting curve shows a constant increase of the emf before the melting process starts. During the melt the slope is decreased. Both parts of the melting curve can be approximated by regression lines, respectively. The intersection point of the two straight regression lines corresponds to the emf of the melting point. The sudden reduced slope indicates the beginning of the melt; the rapid increase of the slope marks the end of the melt. A special feature of the melt by using the integrated fixed-point cells of design A was the dependency of the melting temperature on the heating rate, as presented in Figure 12. Since the hot junction it is not surrounded by the fixed-point material, the measurement is sensitive to the heat flux from the furnace.

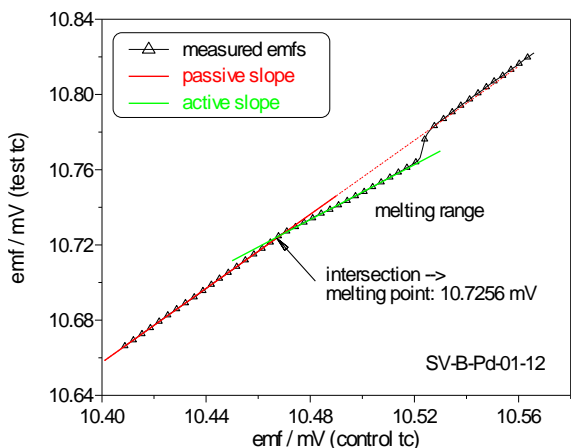


Figure 11 Typical melting curve of palladium

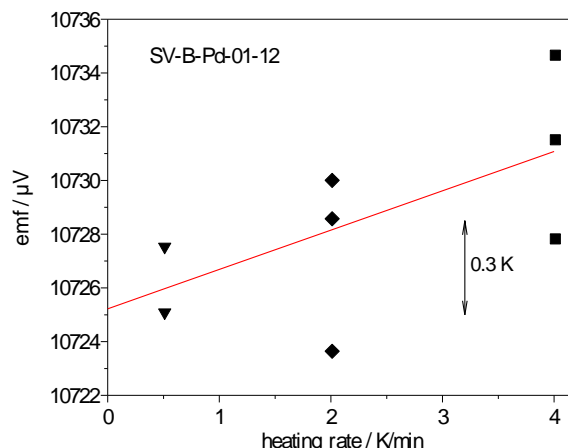


Figure 12 Dependency of the melting temperatures on the heating rate (design A)

The LNE-Cnam designs (RW and PW devices) were tested at the gold, nickel and palladium points. The characteristics of the self-validating thermocouples were evaluated by performing and exploiting melting and freezing point measurements of the self-validating modules, corresponding respectively to the inflection point of the melting plateau and the maximum temperature on the freezing plateau. The melting plateaus of Au, Ni and Pd were clearly observed with both the rolled-wire and the pulled-wire methods using the self-validated thermocouple. However, at the nickel and palladium fixed points, the freezing plateaus were not as repeatable as hoped; moreover the shape of the freezing plateau showed several bumps indicating that different freeze processes were taking place in the independent pieces of metal.

Figure 13 shows the influence of the furnace heating rate on the melting temperature with the palladium in rolled wire and pulled wire configurations. The palladium wire used had a nominal purity of 99.99 %. The influence of the thermal environment was evaluated by adjusting the furnace temperature offset to ± 12 K and changing the heating rate temperature of the furnace (1 K/min, 3 K/min and 6 K/min, successively). The duration of the melting was 1 minute and 3 minutes for heating rates of 6 K/min and 1 K/min, respectively.

The melting plateau was clearly observable, with a melting range of 3 K in the pulled wire configuration and 1 K with the rolled wire devices. The repeatability was within 0.12 K which is satisfactory considering the very small mass of metal (0.1 g and 0.9 g of palladium). To determine and correct the influence of the furnace temperature on the plateau, the equilibrium temperature of the self-validating thermocouple corresponding to adiabatic conditions T_{p0} is determined by the back-extrapolation of the best fit T_p (plateau temperature during melting and freezing) as function of the heating rates of the furnace, shown in Figure 14.

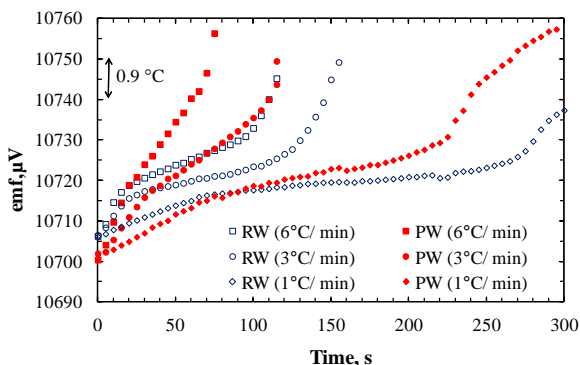


Figure 13 Influence of the heating rate on the melting temperature plateaus within Pd/RW and Pd/PW

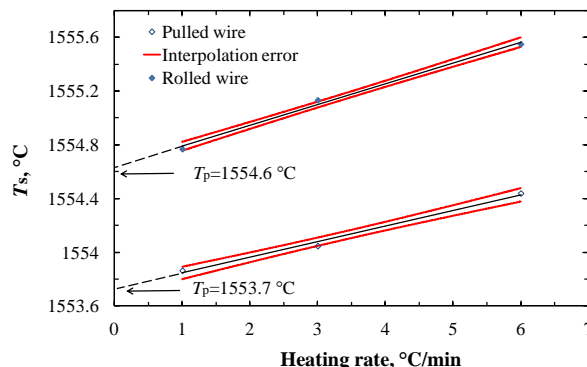


Figure 14 Determination of the plateau temperature in stationary conditions with no heat flow within Pd/RW and Pd/PW

The dependency of the melting temperature on the heating rate is a disadvantage of the method, especially by using the miniature fixed points of design A and the PW devices. Since the hot junction is not or only partially surrounded by the fixed-point material, the measurement is sensitive to the heat flux from the furnace. Therefore, an extrapolation of the results to adiabatic conditions (heating rate of 0 K/min) seems to be necessary. Otherwise, this effect has to be integrated into the uncertainty budget which would increase the combined uncertainty.

To investigate the long-term stability of the integrated miniature fixed points and self-validating structures different heat treatments were applied. The type B thermocouple SV-B-Pd-01-12 with the integrated fixed-point crucible Pd-01-12 (cell design A) was annealed within 5 periods for a total time of about 2133 h at different temperatures. In the first period the thermocouple was annealed for 544 h at 1450 °C, in the second period for 928 h at 800 °C. The thermocouple was cycled over three days in the third period at temperatures of about 1600 °C, i.e. above the melting temperature of palladium for (4 x 6) h and at temperature of 1000 °C (3 x 18 h). In the fourth period the thermocouple was 3 times cycled within of about three weeks at temperatures of 1400 °C for 288 h and at 750 °C for 216 h. The last period was a rerun of the third period; the thermocouple was annealed for 24 h at 1600 °C and 54 h at 1000 °C.

The emfs measured at the external fixed points Ag and Co-C as well as the emfs measured by using the internal Pd fixed point in the course of the annealing procedure are presented in Figure 15. The investigated type B thermocouple SV-B-Pd-01-12 showed an excellent thermoelectric stability in the order of 0.5 K at the freezing point of silver and at the melting point of the Co-C eutectic. In contrast to the unchanged emfs at these external fixed points, the emf measured at the internal Pd fixed point increased strongly. An increase of about 50 μV (temperature equivalent of 4.5 K) was observed over the total annealing time. Therefore, this increased emf must be caused by a change of the melting temperature of the palladium inside the miniature crucible, possibly by a diffusion of platinum from the auxiliary platinum shell into the ceramic crucible. Platinum and palladium form a solid solution with increasing melting temperatures by increasing platinum content.

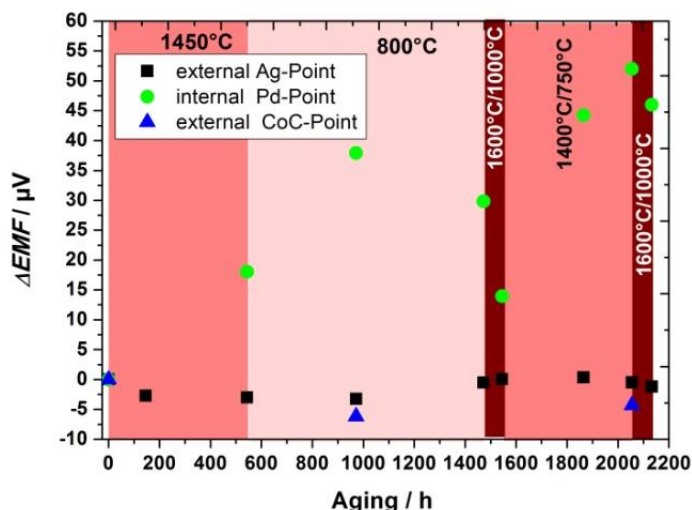


Figure 15 Measured changes of the emfs at the external Ag and Co-C fixed points as well as at the internal Pd fixed point by using SV-B-Pd-01-12.

The two type B thermocouples SV-B-Pt-01-12 and SV-B-Pt-02-12 with integrated Pt fixed points were annealed for 928 h at 800 °C in air before they failed caused by overheating during melting tests of the platinum miniature fixed points. The reference emfs at the external Ag freezing point increased linearly by about 7 μV for both thermocouples (temperature equivalent of 0.8 K) during the annealing procedure. In contrast, the emfs measured by using the internal melting temperatures of Pt exhibited a strong decrease after the first 400 hours of 92 μV (temperature equivalent of 8 K) for the crucible of design B, and 36 μV (temperature equivalent of 3

K) for the crucible of design A. A stabilizing of the emfs at the melting point of Pt (Pt-01-12, design A) was observable after finishing the second annealing period. A further heat treatment of the miniature fixed point Pt-01-12 integrated into a new type B thermocouple over an additional period of about 690 h at temperatures between 750 °C and 1600 °C caused an only slightly increase of the emf at the melting point of Pt by a temperature equivalent of about 1 K.

The type B thermocouple with the integrated fixed-point crucibles PdRW1 and PdRW2 was aged at LNE-Cnam for a total time of about 1150 hours at 1200 °C and cycles around the palladium melting temperature lasted about 100 h. Figure 16 shows the stability of the PdRW2 and PdRW1 modules versus the time spent in the furnace at 1200 °C. The melting points of palladium of the two cells are shown as a function of annealing time. The uncertainty associated with the measurements is of the order of 1.75 K ($k = 2$). The measurement with the reference thermocouple is also shown in the second axis as a function of annealing time. A slight increase in the value of the melting point of palladium (PdRW1 and PdRW2) from 10727 μ V and 10736 μ V to 10741 μ V and 10745 μ V was observed. The same behaviour shows also the reference thermocouple; its value increases from 16126 μ V to 16137 μ V indicating a drift in the furnace temperature. However, this increase of the emf at the melting point of palladium is within the uncertainty. The overall drift of the rolled-wire devices is therefore estimated to be well within 1 K over a period of about 1150 hours at 1200 °C.

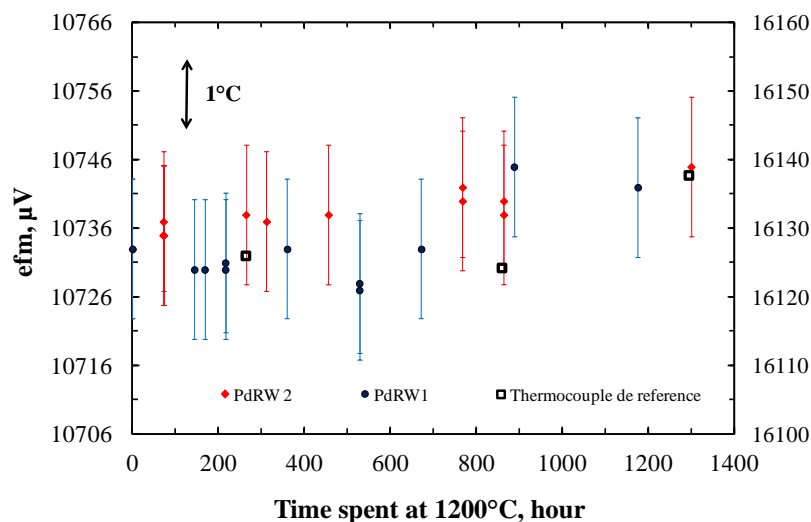


Figure 16 Stability of PdRW1 and PdRW2 devices. The left axis indicates the emf of the type B thermocouple and the right axis indicates the emf of the type S drift-compensation thermocouple

The self-validating concept based on integrated miniature fixed-point cells and self-validating structures usable under oxidising conditions was found to be partially usable to detect drift effects of thermocouples in the order of about 2-3 K by using an integrated platinum fixed point (design A) and the rolled wire and pulled wire devices (Au, Ni, and Pd). The integrated fixed points of design B failed because of mechanically problems (breakage of thin crucible wall made of Al_2O_3). Typical measurement uncertainties ($k = 2$) of the melting temperatures of the used fixed-point materials were in the order of ± 1.5 K.

As a general problem the dependence of the melting temperature on heating rates or offset temperatures was proven. This effect results in a higher measurement uncertainty by a factor of about 2, when not considered by extrapolation of the emfs measured at different heating rates (or different offset temperatures) to adiabatic conditions.

Two combined thermocouple-noise temperature sensors were constructed to investigate the second self-validation concept based on the simultaneous use of noise thermometry to measure temperatures without drift effects. These sensors based on noble metal thermocouples are usable in oxidizing atmospheres. One of the combined thermocouple-noise sensors, RT-B1, consists of two type B thermocouples and the second sensor, RT-S1, consists of two type S thermocouples. They can be used up to temperatures of 1800 °C and 1500 °C,

respectively. A schematic diagram of the combined thermocouple-noise temperature sensors is presented in Figure 17 and a detailed description can be found in [3.6].

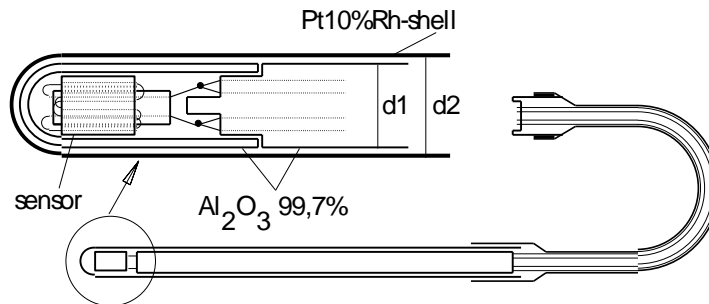


Figure 17 Schematic diagram of a combined thermocouple-noise temperature sensor

First measurements were performed at the freezing points of copper (1084.62 °C) and silver (961.78 °C) to test the accuracy of the combined thermocouple-noise sensors RT-B1 and RT-S1. The mean noise temperatures measured agree to the well-known fixed-point temperatures within about 0.4 K at the freezing point of copper (RT-B1) and within 0.2 K at the freezing point of silver RT-S1. These results demonstrate the suitability of fixed-point measurements as a verification of the accuracy of the combined thermocouple-noise temperature sensors and the noise thermometer electronics (NTEs) used within an uncertainty of at least ± 1 K ($k = 2$).

Afterwards, the thermal stability of the thermocouples of the combined sensors was tested. During the heat treatment of the combined thermocouple-noise sensor RT-B1 at 1450 °C for about 80 hours an increase of the emfs of the two type B thermocouples by about 3.3 μ V (0.35 K) and 4.7 μ V (0.5 K), respectively was found at the freezing point of copper after this heat treatment. This change is less than 0.1 % and is in the order of the measurement uncertainty of the noise temperature, i.e. below its limit of detection.

The combined thermocouple-noise temperature sensor RT-S1 was exposed to two different long term thermal heat treatments at temperatures of about 1100 °C and 1340 °C for 560 hours and 600 hours, respectively. The noise temperatures and the thermocouple temperatures were measured periodically (every 50-100 h). Despite this long term heat treatment at constant temperatures (1100 °C and 1340 °C) over a period of more than 48 days on the whole, no drift of the two type S thermocouples was detectable which indicates their excellent thermoelectric stability. Furthermore, also the measured noise temperatures remain constant and agree very well with the thermocouple temperatures within about ± 0.3 K at 1103 °C. At 1340 °C a systematic difference between the two thermocouple temperatures and the noise temperature of about 2 K was found. This difference remains constant during the first 250 hours of use of the noise thermometer electronics E+H and decreases slightly by about 1 K during the next 350 hours. Nevertheless this apparent drift is within the relative measurement uncertainty of the noise temperature of about (0.1-0.2) % ($k = 2$). Despite the found difference in temperatures between thermocouples and noise thermometer at 1340 °C, the stability of the noise temperature allows to reach the aim of the confirmation and evaluation of drift effects of thermocouples by using noise thermometry.

The accuracy of the noise temperature measurement was also checked by a simultaneous measurement of the radiation temperature by using an optical linear pyrometer LP3. The combined thermocouple-noise temperature sensor RT-B1 was inserted into a bore of a ceramic block in the center of a horizontal high-temperature furnace from one side. Parallel, in a second bore, a black cavity made of platinum was placed at the same axial position like the noise resistor of the sensor RT-B1. This black cavity was used to measure the radiation temperature by the LP3 from the other side of the furnace. The results of the measurements are presented in Figure 18. The error bars corresponds to the statistical uncertainty ($k = 1$) of the noise temperatures (NT).

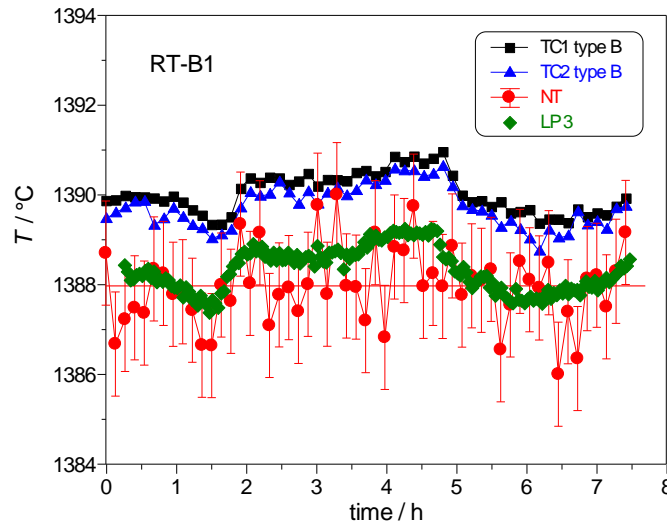


Figure 18 Check of the accuracy of the noise temperature measurement by using an LP3 measuring the radiation temperature independently

The good agreement of the noise temperature and the radiation temperature measured indicates a high accuracy of the absolute noise temperature measurement also at higher temperatures than given by the two fixed points of the ITS-90, the freezing points of copper and silver. The patterns of temperatures measured by the three independent methods show also a high conformity. The uncertainty of the radiation temperature was in the order of ± 1.5 K ($k = 2$).

The self-validation concept for noble metal thermocouples of type S and type B based on the simultaneous use of Johnson noise thermometry to measure absolute temperatures was investigated to validate the thermoelectric stability of thermocouples. Relative measurement uncertainties of the noise temperatures of about 0.1 % are already achievable by using moderate measuring times of about 20 min. This is sufficient to determine and correct for thermocouple drifts in the order of 1-2 K. Under industrial conditions the measurement uncertainty of the noise temperature was found to be larger by a factor of about 2. Suitable measures to reduce the influence EMI, for instance by dimming the heating power during measurement cycles, filtering, or interference suppression by optimised electrical grounding could improve the total uncertainty of the measured noise temperatures to about the same level obtained under laboratory conditions.

The objective for this body of work was to improve in-process contact thermometry by an uncertainty factor of 10 or more through novel self-validating thermometers and practical primary electrical noise thermometry.

The achieved results demonstrate clearly an improvement of the in-process measurement uncertainty of contact thermometers achievable when using integrated miniature fixed-point cells combined with thermocouples or when using noise thermometry as independent method, both applied to evaluate for drift effects of thermocouples used in-process. Especially the combination of W/Re thermocouples with Pt-C and Ru-C miniature eutectic fixed-point cells was successfully tested and allows the correction for drift effects of several degrees within an uncertainty of several tenth of a degree. This proven reduction of the measurement uncertainty corresponds exactly to the aspired aim to reduce it by about a factor of 10 when using self-validating contact thermometry sensors. Relative measurement uncertainties by using the combined thermocouple-noise temperature sensors of about 0.1% were achievable which would be sufficient to determine and correct for unavoidable thermocouple drifts in the order of 1–2 K. Both self-validating contact sensor approaches exhibited the potential to detect and to correct for unavoidable, but also unexpected and random drift effects of thermocouples within an uncertainty less than a factor of 10 of the drift effects itself.

3.3 A methodology for the rigorous determination of ‘reference functions’ for non-standard thermocouple types

High temperature processing is inevitably accompanied by harsh environments and operating conditions that are not conducive to reliable temperature measurement. These conditions are regularly encountered in all industrial sectors that require high temperature measurements (e.g. aerospace/space (about 1300 °C to 3000 °C), nuclear fuel production and essential nuclear safety testing (1800 °C to 2500 °C), refractory metals production (2500 °C), silicon carbide, carbon/carbon composites (to > 2800 °C) and iron, steel, glass and ceramics manufacture (1100 °C to 2000 °C). Many of these industries, because of external competition and growing environmental legislation regulating both emissions (particularly greenhouse gases) and waste, require improved process efficiency/control, which is inextricably linked to improving high temperature measurement.

Thermocouples are often used as control thermometers in industrial processes and in some cases the use of non-standard thermocouple types could be beneficial. However, the lack of reference functions for such sensors has limited their uptake, even though they could be of great use in particular industries. The work undertaken towards this objective has addressed this issue by developing a distributed capability within Europe for the accurate and rapid determination of such reference functions. This would give access to new types of thermocouples that could address current measurement problems.

In this section, the European distributed capability for determining reference functions, with demonstrated traceability to the International Temperature Scale of 1990 (ITS-90), is described and applied to the characterisation of the Pt-40%Rh / Pt-20%Rh thermocouple, referred to hereafter as the “Land-Jewell” thermocouple [6.1].

The Land-Jewell thermocouple is useful for continuous use to 1800 °C and occasional use to 1850 °C. The lower output of the Land-Jewell thermocouple relative to the Type B thermocouple, previously considered a drawback, is mitigated these days by the prevalence of very sensitive digital voltmeters, provided its use is restricted to temperatures in excess of 400 °C. As well as the advantage of its high melting temperature, its high Rh content relative to the letter-designated thermocouples lends it greater stability than the other Pt-Rh thermocouple types above about 1200 °C [6.2] and, in addition, its performance is far superior to the refractory metal W-Re thermocouples [6.3-6.5] under a wide range of conditions [6.6-6.8]. This is because alloys with high Rh content are less sensitive to local changes in Rh content caused by evaporation of the oxides of Pt and Rh which are very volatile at high temperatures [6.9, 6.10].

A number of reference tables for this thermocouple type have been prepared over the years [6.11-6.15]. In practical terms, possibly the most important is that of Bedford [6.15] (which was expressed in terms of IPTS-

48), because the current standard reference tables in ASTM standard E1751-09 [6.16] are thought to be based on it, albeit with modified coefficients to express the reference function in terms of ITS-90 [6.17]. No tolerances on the emf as a function of temperature are specified in the ASTM standard. There is currently no equivalent national, European, or international standard.

There are three compelling reasons for re-visiting the reference function of this thermocouple type. The first reason is that since the earlier determinations, there have been substantial improvements in methods available for calibrating the thermocouples above 1100 °C with the advent of metal-carbon eutectic fixed points [6.18], in particular the Co-C and Pd-C points [6.19-6.22], commonly known as high temperature fixed points (HTFPs), which permit much lower uncertainties than previously obtainable. The second reason is that, to the authors' knowledge, the origin of the coefficients in ASTM standard E1751-09 [6.16], while thought to originate from the measurements of Bedford [6.15], is not documented, either in the standard itself, nor, to the authors' knowledge, in the publicly available literature. The third reason is that in his determination of the reference function [6.15], Bedford took the value of the melting temperature of Pt to be 1769 °C (ITS-48), based on the best available information at the time [6.23-6.25]. To convert from ITS-48 to ITS-90, 2.16 °C should be added to the ITS-48 temperature, which gives 1771.2 °C. Thus the temperature value used by Bedford for the thermocouple Pt wire bridge calibration during the reference function determination [6.15] was effectively 3.0 °C higher than the currently accepted value of 1768.2 °C [6.26]. There is a corresponding knock-on effect over the associated temperature range. The value of the Pd melting temperature used by Bedford was also in error, by about 1 °C. These issues are discussed in detail in the Discussion section below. In the light of the above issue, a modern determination of the reference function might be expected to exhibit a marked deviation from the existing ASTM reference function, becoming higher by several degrees above about 1600 °C. The move to reduce uncertainties at high temperatures is gaining momentum [6.27] and the above questions over the de-facto standard reference function for the Land-Jewell thermocouple justify further investigation.

3.3.1 *Description of the facilities developed for this objective*

Four NMIs participated in this body of work: CEM, LNE-CNAM, NPL, and SMU. In this section the facilities of the participants are described.

3.3.1.1 **CEM facilities**

CEM has facilities for calibrating thermocouples up to 1324 °C using fixed points and up to 1600 °C by comparison to a calibrated radiation thermometer, described in detail in [28].

Above 1000 °C the fixed points used are Cu (1084.62 °C) and the Co-C eutectic (1324 °C). Both fixed point cells are realised in vertical furnaces with temperature uniformity better than 0.5 °C over a length of 200 mm at the Cu point and better than 5 °C over a length of 150 mm at the Co-C point. Both furnaces have three independent heating zones. The furnace used for the Cu point is commercially available, while the one used for the realisation of the Co-C eutectic transition was built in-house. This latter furnace is powered by a DC electrical supply and has four MoSi₂ heater rods in each zone that are symmetrically arranged around a central longitudinal tube of 80 mm diameter. CEM maintains the Cu point used in contact thermometry by means of a group of cells, one of which participated in an international comparison [29], assuring its equivalence to other NMIs. The performance of the group is monitored by using a Type R reference thermocouple. The expanded uncertainty (i.e. $k = 2$) in the realisation of the Cu point is 0.17 °C. The Co-C cell has an expanded uncertainty in its realisation of 0.5 °C and its melting temperature has been determined with a standard radiation thermometer calibrated according to the ITS-90 [30].

To determine the relationship between temperature and emf (electro-motive force, or thermovoltage) of a thermocouple by comparison to a radiation thermometer, a three-zone horizontal furnace, constructed in-house, is used [28]. This is also powered by a DC electrical supply, and also uses MoSi₂ heating resistors. Inside the furnace is an alumina tube containing a graphite blackbody (BB). The BB has a cylindrical cavity of length 100 mm and diameter 10 mm. The cavity terminates with a conical geometry at the back wall. The thermocouple is inserted at the rear part of the furnace, so that the measurement junction of the thermocouple touches the rear part of the graphite BB cavity. The traceability to ITS-90 is assured by means of a standard monochromatic radiation thermometer VEGA TSP2.11 (900 nm) focused on the aperture of the BB. The standard radiation thermometer is calibrated at the Cu FP and characterised in terms of wavelength, linearity and size of source effect (SSE). The thermometer target is 1.05 mm x 1.40 mm at a distance of 700 mm. In this way, taking into account the calculated emissivity of the BB, the temperature of the thermocouple may be deduced. The uncertainty in the temperature assigned to the thermocouple via the comparator ranges from 0.5 °C at 900 °C to 1.1 °C at 1600 °C ($k = 2$).

The measurement of the thermocouple emf is performed by using an automated system composed of a 8 ½ digit voltmeter (HP 3458), a DC voltage standard (Fluke 732 B) and a voltage divider (Fluke 752 A). This system allows the daily calibration of the multimeter thus achieving its best performance. Combining uncertainties due to voltmeter calibration, linearity, parasitic voltages, and scanner calibration yields an expanded uncertainty for the thermocouple measurements of about 0.52 \square V. However, usually the most important source of uncertainty when actually using thermocouples arises not from the measurement system but from the thermoelectric inhomogeneity of the thermoelements.

The latter source of uncertainty means that any high precision determination of thermocouple reference functions requires the quantification of the effects of thermoelement inhomogeneity. This is usually determined by locally changing the temperature profile along the length of the thermocouple, by heating or cooling, while maintaining the measurement junction and reference junction at constant temperature (usually the temperature of melting ice, 0 °C). The temperature gradient region is moved along the length of the thermocouple, whereupon local thermoelectric inhomogeneities can be detected from the changes in emf as a function of thermocouple position. CEM has two methods available. The first method is performed at about 200 °C using a stirred oil bath with vertical uniformity better than 0.05 °C. An automatic system for withdrawing the thermocouple from the bath, and a Keithley 2000 voltmeter with a resolution of 0.1 μ V, are also used to record the change in emf. If it is considered necessary, for instance in cases in which the thermocouples have low sensitivity at 200 °C, it is possible to use a silver fixed point cell (961.78 °C) which provides a zone of uniform temperature during the freeze. The maximum immersion depth is 400 mm for the oil bath and 150 mm for the silver fixed point.

The maximal variation of the emf over the distance where the measurement junction is at constant temperature is taken to be the width of a rectangular distribution of values associated with the uncertainty due to thermoelectric inhomogeneity. For Types R and S thermocouples, it is accepted that the inhomogeneity measured at one temperature, expressed as the fraction of the total emf at this temperature, is representative of the inhomogeneity at others temperatures [31]. This principle has also been employed for Pt/Pd thermocouples [20], and it is assumed in this work to be equally applicable to Land-Jewell thermocouples.

3.3.1.2 LNE-CNAM facilities

Above 1000 °C, LNE-Cnam has developed a series of high temperature fixed-points (HTFPs) up to a temperature of 1500 °C suitable for thermocouple calibration, as well as a number of HTFPs up to a temperature of 1953 °C which are used for radiation thermometry but can be adapted for thermocouple calibration. The thermocouple HTFPs are based on the Co-C (1324 °C) and Pd-C (1492 °C) melting points [33-36] and were developed in the Euramet 857 project [33,34]. With the aim of covering the temperature range up to 2000 °C, LNE-Cnam has recently developed new HTFPs including the Cr-C eutectic and peritectic melting points (respectively 1742 °C and 1826 °C) [19, 37], and the Ru-C eutectic melting point (1953 °C) which are traceably calibrated [39]. However, due to technical problems with the furnace used for realising these fixed points, the LNE-Cnam measurements in this article were restricted to the wire bridge calibrations using Au, Pd, and Pt points, and the freezing point of silver using a conventional tube furnace. The uncertainty of calibration ($k = 2$) of Land-Jewell thermocouples ranges from 0.7 °C at the silver freezing point to 2.1 °C at the Pt wire bridge point. The thermoelectric inhomogeneity was characterised by immersion measurements in a silver freezing point cell.

3.3.1.3 NPL facilities

NPL has facilities for calibrating thermocouples up to 1500 °C using fixed-point cells, and up to 1800 °C using the wire-bridge method.

Above 1000 °C, the pure metal fixed point of Cu and the HTFPs of Co-C and Pd-C are used. These are realised in vertical furnaces, with a thermal uniformity of 1.6 °C, 0.5 °C, and 0.8 °C over 80 mm for each cell respectively. For the Cu point, an Elite Thermal Systems (UK) three-zone furnace is used. For the HTFPs, Carbolite (UK) three-zone furnaces are used. A traceable temperature is assigned to each of the HTFPs by certification against a radiation thermometer (calibrated in terms of the ITS-90, and regularly checked against the Cu point). The standard uncertainty contributing to the calibration uncertainty budget for impurity effects on the realisation of the fixed-point temperature is taken to be 0.01 °C for each of the cells. The standard uncertainty on the assignment of a melting temperature to the cell by radiation thermometry is taken to be 0.22 °C (0.32 °C) for the Co-C (Pd-C) cell. Both Co-C and Pd-C cells (and the Ag cell, also used) have been shown to be consistent via intercomparisons between NPL, LNE, NMIJ, and PTB performed within the Euramet 857 project [33,34].

At NPL, the wire-bridge method is used with pure Pd and pure Pt wires (in air) to realise the temperatures 1553.5 °C and 1768.2 °C, respectively. A custom-built Elite Thermal Systems single-zone furnace is used, which has MoSi₂ heaters and a hot zone with a uniformity of 0.5 °C over approximately 20 mm (at the Pt melting temperature). As the melting temperature of Pd is close to the melting temperature of Pd-C, only the Pt wire-bridge point was used in this study. The expanded uncertainty of the Pt melting temperature is 0.5 °C ($k = 2$).

In addition to these fixed points, the NPL national reference standard cells of Zn (419.527 °C), Ag (961.78 °C) and on one occasion both Sn (231.928 °C) and Al (660.323 °C), were also used.

The measurement of the thermocouple emf was performed by using an automated system composed of a Keithley 2182A nanovoltmeter (resolution 10 nV) and in-house software for recording the output of the thermocouple every 10 s. The maximum change in thermocouple output between 0 mm and 80 mm from full immersion during the Ag freezing point realisation is used to represent the uncertainty associated with thermoelectric inhomogeneity. The typical expanded uncertainty of calibration of Land-Jewell thermocouples is found to range from 1.7 °C at the Sn point, to 4.3 °C at the Pt point.

The usual facility for determining thermocouple inhomogeneity at NPL consists of a stirred oil bath at 150 °C. This has an immersion depth of 580 mm and a uniformity of 12 mK or better. To perform the test, each thermocouple is immersed in the oil bath and allowed to reach thermal equilibrium. The thermocouple is withdrawn and immersed with steps of typically 10 mm, using an automated linear translation stage to ensure repeatability. Note that because the output and sensitivity of the Land-Jewell thermocouple is very small at 150 °C (65 µV and 0.5 µV / °C respectively), the method of immersion in the Ag cell is preferred for quantifying the inhomogeneity; the oil bath can give only a qualitative indication of the thermocouple, albeit over a much longer distance than available with the fixed point method.

3.3.1.4 SMU facilities

SMU is capable of calibrating thermocouples up to 1200 °C by comparison to a calibrated radiation thermometer. The furnace used for calibration is a commercially available spherical furnace with metal resistance heating elements. The furnace has two openings: one for insertion of the thermocouple under test, and the other for the radiation thermometer. The setup was arranged such that the radiation thermometer had a line of sight to the tip of the thermocouple under test.

The thermocouple measurement junction was placed at the centre of the spherical furnace where the temperature uniformity and stability is highest. A ceramic BB cavity is placed in close proximity to the measurement junction of the thermocouple. The BB cavity was cylindrical with an overall length of 25 mm, an inner diameter of 5 mm, and wall thickness of 1.7 mm. The BB cavity emissivity was well characterised. Traceability to ITS-90 was assured through the use of a photoelectric pyrometer with an effective wavelength 952 nm and a measuring spot of diameter 0.7 mm. The photoelectric pyrometer was calibrated at the Au fixed point and characterised in terms of wavelength, linearity and SSE. The uncertainty in the temperature assigned to the thermocouple via the comparator between 900 °C to 1200 °C is 1.3 °C ($k = 2$).

The measurements of the thermocouple emf were made by an automatic recording system which consists of a calibrated 6 ½ digit multimeter HP 34401A, recording software and a PC. The thermoelectric homogeneity was measured with a stirred oil bath with overall immersion depth 550 mm and vertical temperature uniformity better than 80 mK, the result being used as a contribution to the final uncertainty budget.

3.3.1.5 Determination of the Pt-40%Rh versus Pt-20%Rh thermocouple reference function

It has been observed that the thermoelectric stability of Pt-Rh alloys used in air at high temperatures is independent of wire diameter [6,7,41], and hence in principle the reference function could be determined with any diameter wire. For these measurements, a wire diameter of 0.5 mm was used as the best compromise between ease of use with the available facilities, and robustness. The Pt-40%Rh and Pt-20%Rh wires were purchased from Johnson Matthey. The wires were cleaned with ethyl alcohol and annealed electrically for 30 minutes, then inserted in a twin-bore 99.7 % pure alumina tube (pre-baked in air at 1500 °C for 24 hours) of outer diameter 4 mm, bore inner diameter 1.2 mm, length 710 mm. The ends of the wires were directly welded to form the measurement junction; the wires protruding from the alumina insulator were individually encased in PTFE sleeving. The wires emerging from the sleeving were connected to copper wires by twisting together, and placed in a glass tube to form the reference junction. The thermocouple was protected by placing it in a one-end closed alumina sheath of inner diameter 5 mm, outer diameter 7 mm, length 700 mm.

In total, four thermocouples were prepared, designated TC3, TC4, TC5, and TC6, for two phases of reference function determination (by calibration) amongst the partners. Phase 1 comprised TC3 and TC4, both made of wires from the same batch. Phase 2 comprised TC5 and TC6, both made of the wires from the same batch, this batch being different to that for Phase 1. The Phase 1 thermocouples were calibrated by each participant in the following order: NPL #1, CEM, NPL #2, SMU, LNE-CNAM, NPL #3. The thermocouples were sent between the participants by courier. The process was repeated for the Phase 2 thermocouples, with a different order to accommodate availability of resources: CEM, SMU, NPL #1, LNE.

Calibration facilities available, the temperature ranges, and uncertainty on the calibration measurement are summarised in Table 2.

Table 2 summary of calibration facilities used by the partners: type of calibration apparatus (FP: fixed point, Comp: comparison with reference thermometer), temperature T, and overall uncertainty of the thermocouple calibration U, including thermoelectric inho

NPL				CEM				SMU				LNE-Cnam			
Type	T / °C	U / μV	U / °C	Type	T / °C	U / μV	U / °C	Type	T / °C	U / μV	U / °C	Type	T / °C	U / μV	U / °C
Sn FP	231.93	1.1	1.7	Cu FP	1084.62	1.7	0.5	Ag FP	961.78	2.1	0.8	Au FP	1064.18	2.3	0.7
Zn FP	419.53	1.2	1.1	Co-C FP	1324	2.7	0.7	Comp	900 - 1200	4.6	1.3	Pd FP	1553.4	6.7	1.5
Al FP	660.32	1.8	0.9	Comp	1200 - 1550	3 - 4.5	0.8 - 1.1					Pt FP	1768.2	9.6	2.1
Ag FP	961.78	3.7	1.3												
Cu FP	1084.62	3.7	1.2												
Co-C FP	1324.29	6.7	1.7												
Pd-C FP	1491.5	8.5	2.0												
Pt FP	1768.2	19.3	4.3												

To monitor the stability of the thermocouples, where possible, each partner performed measurements at the silver point before or after the calibration measurements. These measurements are shown in Figure 19. Emf at the freezing point of silver as measured by each partner during the calibration measurements. It can be seen in Figure 20 that the thermocouple stability as measured at the silver point is within about 1 °C with no evidence of a systematic drift of emf.

The calibration measurements performed by each partner are shown in Figure 20, expressed in terms of the difference between the measured emf and the emf given by the reference function in ASTM E1751-09. Figure 20 shows a discrepancy in the measurements between about 1500 °C and 1750 °C, for both the Phase 1 and Phase 2 thermocouples, indicating an inconsistency between the current measurements and the ASTM reference function.

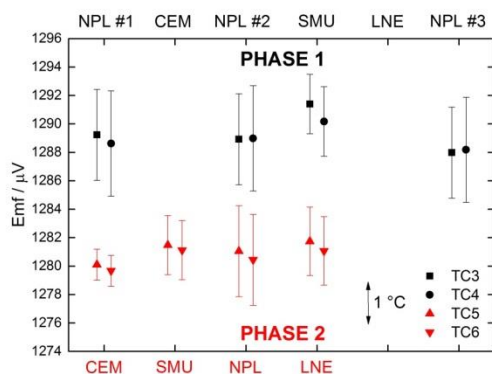


Figure 19 Emf at the freezing point of silver as measured by each partner during the calibration measurements.

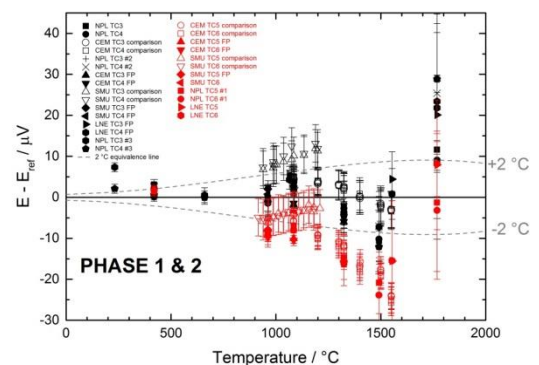


Figure 20 Difference between measured emf and the ASTM reference emf, showing a sharp increase in emf above about 1500 °C

To determine a draft ‘reference function’ based on the four thermocouples, all data were combined, and a 5th order polynomial was fitted to the ensemble using the least-squares method, weighted by the uncertainty of the measurements, as shown in Figure 3. The best-fit polynomial has the form

$$E = a_0 + a_1T + a_2T^2 + a_3T^3 + a_4T^4 + a_5T^5$$

where T is the temperature in units of °C, E is the emf in units of μV, and the best-fit coefficients a are given in Table 3. The fitted reference function is shown in Figure 21, together with the combined calibration data. The residuals of the fit are shown in Figure 22. The significantly higher emf at the Pt melting temperature,

amounting to an equivalent temperature of between 2 °C and 6 °C (Figure 19), compared with that of the published reference function in ASTM E1751-09 is clear in Figure 23 **Error! Reference source not found.**

Table 3 Polynomial coefficients of the best-fit reference function (current work).

a_0	0
a_1	0.491576643543637
a_2	$-3.21606929140911 \times 10^{-4}$
a_3	$1.9770622937919 \times 10^{-6}$
a_4	$-8.87382672627336 \times 10^{-10}$
a_5	$1.34438698221336 \times 10^{-13}$

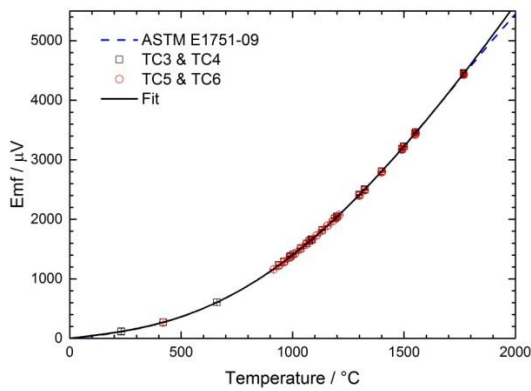


Figure 21 Measured emf as a function of temperature for Phase 1 (TC3 and TC4), black squares, and Phase 2 (TC5 and TC6), red circles. Fitted reference function, black line. ASTM E1751-09 reference function, blue dashed line. Note the good linearity above about 13

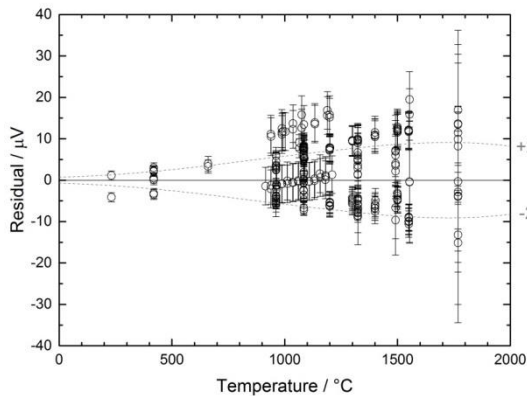


Figure 22 Residuals of the least-squares fit to obtain the reference function.

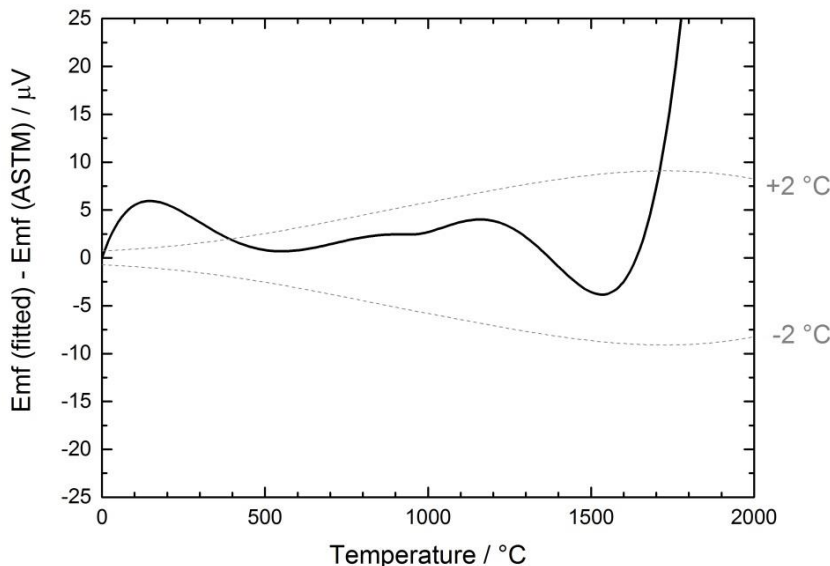


Figure 23 Difference between the current reference function and the ASTM reference function.

3.3.1.6 Ramifications of the findings (progress beyond the state of the art)

Given their importance in the current investigation, some consideration is given to the value of the melting temperatures of pure palladium and pure platinum. All uncertainties referred to in the following discussion correspond to coverage factor $k = 2$ unless stated otherwise.

3.3.1.6.1 Melting temperature of palladium

To convert IPTS-68 temperatures to ITS-90 temperatures at about 1550 °C, 0.47 °C should be subtracted from the IPTS-68 value. Bedford et al. [6.26] provide an ITS-90 value of 1554.8 °C ± 0.1 °C for the melting point of palladium when oxygen is not present. However, commonly the melting point is realised in air; in this case, the high solubility of oxygen in palladium results in a decrease of the melting temperature. Jones and Hall [6.42] determined the IPTS-68 melting temperature in argon to be 1555.0 °C ± 0.4 °C, and in air to be about 1553.6 °C (1553.1 °C on ITS-90), suggesting a depression of about 1.4 °C due to the influence of oxygen. Coates et al. [6.43] obtained an IPTS-68 value of 1555.4 °C ± 0.2 °C ($k = 3$). Jones [6.44] obtained an IPTS-68 temperature of 1555.1 °C ± 0.3 °C. Edler [6.45] found that the melting point in air was lower than that in argon by 1.3 °C ± 0.2 °C, which corresponds to the generally accepted difference of 1.4 °C within uncertainties. The value used for this investigation (in air) was thus 1553.4 °C ± 0.2 °C, based on Bedford's value of 1554.8 °C in argon [6.26]. Note Bedford's value [6.11] is the weighted mean of the values reported in [6.42-6.44].

3.3.1.6.2 Melting temperature of platinum

To convert IPTS-68 temperatures to ITS-90 values at about 1770 °C, 0.58 °C should be subtracted from the IPTS-68 value. Early determinations of the melting point of platinum in the 1930s by Schofield at NPL [6.23], Roeser et al. at NBS (now NIST) [6.24], and Hoffmann and Tingwaldt at PTR (now PTB) [6.25] have been shown to be consistently higher by about 3 °C than more recent determinations, if all temperatures are expressed in terms of ITS-90. This was brought to light by the measurements of Quinn and Chandler at NPL [6.46] which were later retracted and replaced with [6.47]. Further measurements were performed by Jones

Report Status: PU Public

and Tapping at NML (now NMIA) [6.48], Kunz and Lohrengel at PTB [6.49], Lanza and Ricolfi at IMGC (now INRiM) [6.50], and Bezemer and Jongerius at Utrecht University [6.51]. The various determinations to date are summarised in Figure 24.

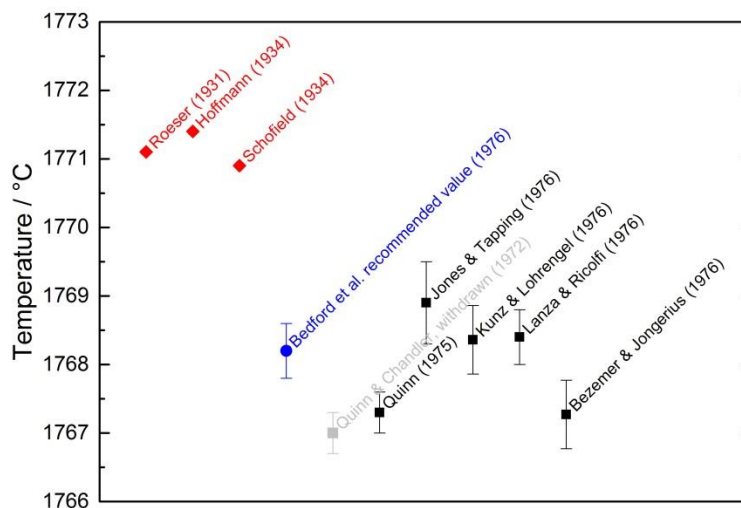


Figure 24 Determinations of the melting temperature of platinum and their uncertainties ($k = 2$), where evaluated. All temperatures are in terms of ITS-90

The current de-facto reference melting temperature is based on the survey of Bedford et al. (IPTS-68) [6.52] which was later revised for the ITS-90 [6.26], although the IPTS-68 value given in [6.52] is not consistent with the cited references [6.46-6.50], even if the retracted value of Quinn and Chandler [46] is omitted. This anomaly is carried forward in the ITS-90 revision of Bedford et al. [6.26]. In this study, the arithmetic mean of the values of [6.47-6.51] is taken, giving an ITS-90 value of 1768.1 °C. Note that this is 0.1 °C lower than the recommended value of Bedford et al. [6.26], perhaps due to the inclusion here of the value of Bezemer and Jongerius [6.51] which is not cited in [6.26] despite being available at that time. The uncertainty on this value is taken to be the expanded uncertainty divided by the square root of the number of values used to inform the mean, which yields 0.5 °C. In this investigation, the melting temperature of Pt is taken to be 1768.2 °C \pm 0.5 °C (coverage factor $k = 2$), based on the recommended value of Bedford et al. [6.26].

Note that in his determination of the reference function of Land-Jewell thermocouples in 1965 [6.15], Bedford took the value of the melting temperature of Pt to be 1769 °C (ITS-48), based on the best available information at the time [6.23-6.25]. To convert from IPTS-48 to ITS-90 at this temperature, 2.16 °C should be added to the IPTS-48 temperature, which gives 1771.2 °C. Thus the value used by Bedford in the reference function determination [6.15] was effectively 3.0 °C higher than the currently accepted value of 1768.2 °C [6.26]. This means that the emf recorded at the Pt point by Bedford [6.15] was too low by an amount corresponding to about 3 °C, with a corresponding effect on the associated temperature range, i.e. above about 1500 °C. Thus, a modern determination of the reference function should be higher than the existing ASTM reference function around 1770 °C by an equivalent of about 3 °C, which is what we observe. A similar but opposite argument applies to the melting temperature of Pd, where 1.83 °C should be added to the IPTS-48 temperature to convert to ITS-90, making the value of 1553.8 °C used by Bedford for the reference function determination [6.15] (for Pd melting in argon atmosphere) 1.0 °C lower than the currently accepted value of 1554.8 °C [6.26]. This means that the uncertainty associated with the Bedford reference function may be higher than previously thought [6.15] above 1500 °C, and this is in fact suggested by the findings of this study.

3.3.1.6.3 Summary

In summary, the key output of this objective is a European distributed capability for determining reference functions, with traceability to the International Temperature Scale of 1990 (ITS-90). This has been applied to the characterisation of the Pt-40%Rh / Pt-20%Rh (Land-Jewell) thermocouple. The cohort comprised four thermocouples from two separate batches, all from the same supplier. An example reference function

was generated, and some disagreement between these results and the current standard reference function given in ASTM E1751-09 was observed. This disagreement is thought to arise from the values of the Pd and Pt melting temperatures that were used in 1965 for the generation of the reference function in the de-facto standard ASTM E1751-09, which were too low by 1 °C (Pd) and too high by 3 °C (Pt). The Land-Jewell thermocouple is of great utility above about 1500 °C and the current work lays the ground for a revised determination of the reference function for this thermocouple type, and future development of an international standard reference function.

The objective for this body of work was to develop a European facility to rapidly determine the reference function of non-standard thermocouples so that said sensors are easily accessible to industry.

The activities and results outlined above have definitively contributed to the objective of establishing a European facility for rapid characterisation of high temperature thermocouples and other sensors. This characterisation takes the form of a reference function (rigorous determination of the relationship between the thermocouple voltage and the temperature) by multiple NMIs. The establishment of independent, complementary calibration techniques at the different NMIs, and a practical means of drawing all the results together, along with a practical demonstration of the facility using the Pt-40%Rh vs. Pt-20%Rh thermocouple, represents achievement of the technical objective.

3.4 Traceable and accurate radiation measurement techniques for in situ surface high temperature measurements above 1000 °C

The aim of this objective was to provide solutions to known issues in radiation thermometry (e.g., emissivity and background reflections) that are significantly limiting the accuracy and achievable measurement uncertainty of non-contact temperature techniques for industrial applications.

The activities within this body of research involved the development of various techniques for temperature and emissivity measurements and the investigation of sources of measurement uncertainty, like size-of-source effect and geometries of surfaces under measurement.

3.4.1 UV-multiwavelength techniques for simultaneous temperature and emissivity measurements

Multi-wavelength thermometry is essentially based on the measurement of the radiance of a source at several wavelengths. The approach is very attractive since from the series of multi-wavelength measurements the surface temperature and emissivity of the sample can be simultaneously determined. This measurement technique can be implemented in various hardware configurations to improve the accuracy. The current state-of-the-art hardware implementation uses a linear position-sensitive detector array (PDA) or CCD array detectors in conjunction with a spectrally-selective device (e.g., a monochromator or a spectrograph). This implementation allows a high degree of flexibility both in terms of the numbers and position of the working wavelength bands. However, in practice these advantages are not sufficient to make the multi-wavelength approach reliable for operations in the VIS-NIR (e.g., in the spectral range useful for temperature measurements around 1000 °C or less). Operating in the typical wavelength band of 0.65 μm - 0.95 μm makes the instrument highly sensitive to measurement noise and model errors (errors arising from an incorrect assumption of the behaviour of the spectral emissivity).

INRIM has performed rigorous mathematical simulations and has shown that employing a multi-wavelength approach in the UV region could lead to a significant potential reduction in uncertainty. The conclusion from the simulation activity is that extending the operating wavelengths down to 0.35 μm considerably reduces the influence of measurement noise and model errors. Errors due to random noise can be reduced by a factor of more than 20 when the emissivity can be modelled with a 2nd order polynomial. The model errors are largely dependent on the equation used in the model and consequently a detailed investigation was carried out with both real materials and some fictitious linear equations. The reduction of the model errors when the measuring system was operated to the 0.35 μm - 0.95 μm band was consistent with all equation models.

INRIM has developed a prototype measurement set-up to validate the outcome of the simulation and demonstrate the feasibility of simultaneous determination of the surface temperature and emissivity. At the core of the multi-wavelength measuring system are two commercially-available devices, a spectrograph Horiba Scientific model MicroHR-Auto and a TE-cooled CCD detector Horiba Sincerity 1024 x 256, coupled together. The measuring system has undergone a fully metrological investigation both in terms of optical and electronics performances. Consequently, the MWT setup was used in a measurement comparison using a particular artefact – Inconel 600. Results of the temperature and emissivity measurements of Inconel 600 sample are presented in Table 4 and Table 5. For the temperature measurement, the estimated measurement combined standard uncertainty is 5.5 °C ($k=2$). For the emissivity measurement, the estimated standard uncertainty is 0.036 ($k=1$). From Table 4, the temperature reading of the MWT setup is compared with the reading from standard reference radiation thermometer (SRT) at INRIM. The values obtained by MWT setup are in good agreement with the reading of the SRT (except at the 880 °C temperature setpoint where the MWT setup is no longer operating optimally). The absolute temperature difference between two readings is within the uncertainty of the MWT setup.

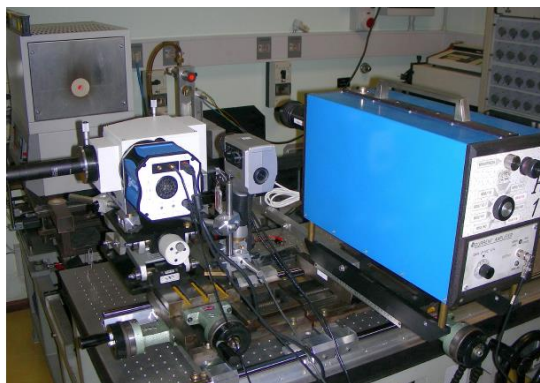


Figure 25 UV-multiwavelength measurement setup developed by INRIM.

Table 4 Temperature measurements of Inconel 600 sample using the multiwavelength thermometry method

Measurement run	ts = 880 °C		ts = 900 °C		ts = 920 °C	
	SRT (°C)	MWT (°C)	SRT (°C)	MWT (°C)	SRT (°C)	MWT (°C)
1	882.3	887.4	900.6	905.1	920.5	924
2	882.5	890.7	901	903.5	921.1	922.1
3	880.6	883.5	901.8	905.1	921.4	920
4	881.4	886.8	902.4	901.3	922.4	925
5	881.7	885.5	902.8	899.6	922.8	923
average	881.7	886.8	901.7	902.9	921.6	
std.	0.8	2.7	0.9	2.4	0.9	922.8

Table 5 Derived spectral emissivity of the Inconel 600 sample at 900 °C from the MWT method.

Wavelength (nm)	Emissivity, ϵ
500	0.940
550	0.935
600	0.930
650	0.925
700	0.920
750	0.915
800	0.910
850	0.905
900	0.900
950	0.895

3.4.2 Determining the size-of-source effect using scanning method

Size-of-source effect (SSE) is one of the significant contributors to the measurement uncertainty in radiation thermometers and often overlooked by non-specialist users. This effect is the result of diffraction, non-uniformity of the radiation source, and the limitations imposed by the field of view of the thermometer. With the significant change of the output signal due to the source aperture, radiation thermometers (RTs) which are not properly calibrated in terms of the SSE contribution can produce large deviations from the true temperature of the source. This leads, consequently, to erroneous and unreliable temperature measurements. Traditionally, there are two methods used to determine the SSE: the direct method and the indirect method which involve the use of sets of circular apertures of different sizes. The implementation of these methods for SSE

determination is extremely time consuming. Recently, a scanning method was proposed. This method is based on scanning the RT across an aperture (a narrow slit situated at the source plane) and determining the SSE from the residual signal. The obvious advantage of this scanning method compared with the traditional methods is faster SSE measurement time. Additionally, this method can cover much wider angles compared with the other two methods. VSL studied the main factors of this scanning method that significantly influence the RT reading. It has been established that the slit position and size can significantly affect the results obtained by the scanning method. With the proper tuning of the position and width of the slit, the SSE behaviour obtained with the scanning method resembles to the SSE obtained by the direct method (Figure 26). This conclusion regarding the similarity of measured SSE of the direct and scanning methods apply primarily to the RT used in the study and may vary with other direct reading radiation thermometers.

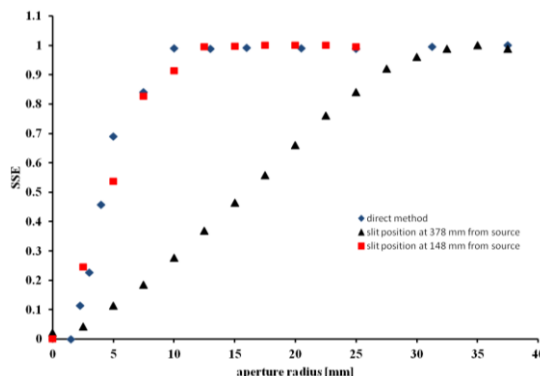


Figure 26 Comparison of the resulting SSE from: (1) direct method (blue diamond) and scanning method using a 36mm slit situated at a distance of (2) 148mm (red squares) and (3) 378mm (black triangles) from the source

3.4.3 Best measurement practice for using gold-cup radiation thermometers on curved and sloped surfaces

Gold-cup radiation thermometers (Figure 27a) have proven useful in industrial applications. These devices work by bringing a reflecting cup (often a hemisphere) close to the surface to be measured. Pseudo-blackbody radiation is established in the cup, negating the emissivity of the surface and thereby facilitating reliable temperature measurement. However, the results provided by this type of radiation thermometer is highly influenced by the surface geometry and tubular and sloping surfaces are commonly encountered in various processing industries. VSL has built a facility (Figure 27b-d) where gold-cup radiation thermometers can be characterised properly with different surface geometries (Figure 27c-d). Characterisation results have shown that the uncertainty associated with the measurement on a curved surface at a temperature of 700 °C could be as high as 3.5 °C ($k = 2$), which accounts for more than half of the total uncertainty (6.1 °C) of the measurement. For sloping surfaces, an uncertainty contribution of the surface geometry amounts to 0.4 °C (at a maximum angle of 20°), with the overall uncertainty of 5.4 °C. These results show that gold-cup radiation thermometry is relatively insensitive to slightly sloped surfaces but is strongly affected by curved surfaces. Additionally, VSL has prepared a report describing the best practice guide in using gold-cup RT on curved and sloping surfaces. This will facilitate the proper use of the instrument to end-user in industrial temperature measurements when confronted with curved and sloped surface geometries.

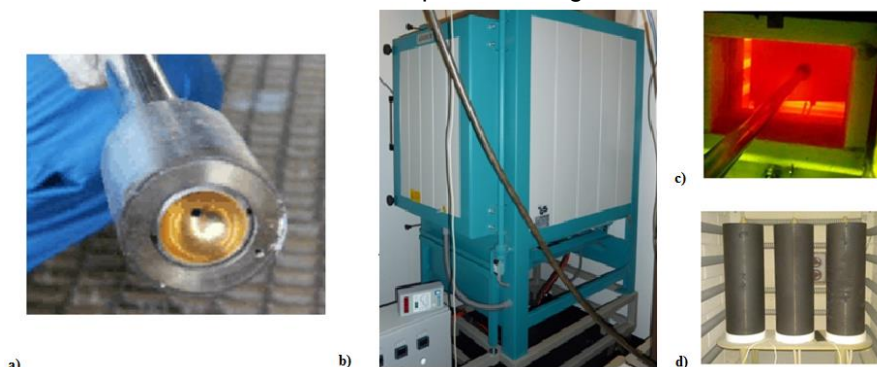


Figure 27 Facility for industrial size-of-source characterization developed at VSL.

3.4.4 Absolute thermovisual characterisation of thermal imager

Thermal imagers (TI), particularly those that are based on focal plane array technology (FPA), are gaining wider acceptance in industrial noncontact temperature measurements due to their capability in providing a much faster two-dimensional temperature map of a surface under test in a single measurement compared with the older type scanning thermal imagers. There is a growing interest in using these devices to make absolute temperature measurements, as well as qualitative two-dimensional thermal distribution of a large surfaces under test. However, the proper characterization of TI's, in general, is far more complex compared with single spot RT's. Inherent in the calibration complexity are the contributions of the extraneous radiation sources (e.g., background radiation from the surrounding, reflected radiations from surrounding and onto the surface under test, etc), and SSE. Furthermore, every individual pixel element in the TI sensor has an inherent electronic noise. For accurate quantitative temperature measurement, each sensor noises needs to be fully accounted for, unlike in single spot RTs which have a single detector element. For thermal imagers, temperature calibration alone is far from adequate in providing a reliable measurement reading from such instruments. Other important parameters of TIs which are regularly included in their characterization include noise-equivalent temperature difference (NETD), thermal resolution, spatial non-uniformity, thermal contrast among others.

VSL has adopted a characterisation method (so called triangle orientation detection (TOD)) for forward-looking infrared thermal imagers, which is successfully utilised in the technical field of infrared target detection and recognition. VSL investigated the usefulness of this technique in absolute thermo-visual calibration of thermal imagers. The common approach for temperature calibration of a thermal imager is with the use of a large area blackbody source that almost fills the field of view of the imager. Different from this common calibration approach, the proposed triangle pattern recognition method uses a large-area source with a predefined triangular pattern at the centre (Figure 28a). The basic idea is to have the temperatures of the reference source and background controllable and accurately measurable. The radiation from the reference source (blackbody) is confined within the area of the triangular pattern, while outside this triangle is considered the background. This target source can be easily realised using a thin plate with a cut-out equilateral triangle pattern at the centre of the plate. VSL has developed a prototype characterization source to realise the absolute thermovisual calibration of a FPA uncooled microbolometer TI (Figure 28b). With the thermal imager, we measured and recorded the spatiotemporal temperature distribution of the target source (reference and background) for each triangular pattern with respect to the size, orientation and thermal contrast (temperature difference between reference and background). From this information, we then determine the various imager parameters such as surface temperature non-uniformity, spatial resolution, and noise-equivalent temperature difference (NETD), temporal stability, etc. The main advantage of this method is that it provides a comprehensive calibration of thermal imagers with less user-intervention during the measurement. This can be fully automated thereby shortening the measurement time. An example of the thermal contrast, as function of the reference source size, achievable for the thermal imager we calibrated is shown in Figure 29. The determined NETD for this type of imager is 80 ± 10 mK.

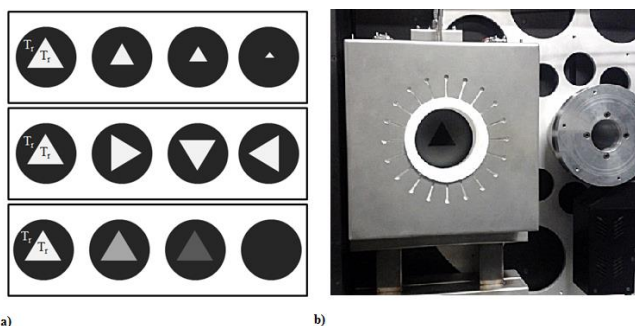


Figure 28 Absolute thermo-visual calibration of thermal imager using the a) concept of triangular pattern recognition. A prototype calibration source based on this approach has been developed and is shown in b).

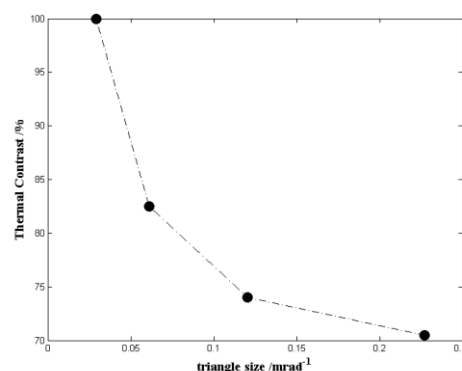


Figure 29 Thermal contrast as function of the triangular size of the reference source obtainable using a FPA uncooled microbolometer imager.

3.4.5 *Improvement and validation of active two-colour laser-based radiation thermometer*

Active two-colour laser radiation thermometer (LART) is based on modulated photothermal effect. Photothermal effect is the conversion of the photon energy from a light source irradiating a surface of a sample into thermal energy of the sample. Due to this absorption of photon energy, the temperature of the sample correspondingly increases. This temperature increase in turn generates various detectable signals such as surface reflectivity, acoustic and thermal waves, and thermal emission. The temperature of the sample is perturbed by an external radiation source, typically a laser. This perturbed thermal signal depends on the true temperature of the sample as well as on the induced modulated temperature variation created by the external source. The sample temperature can be inferred from the detected signal.

VSL has improved a previously built prototype active two-colour LART (Figure 30) to allow it to be useful for in-situ industrial temperature measurements. The fundamental improvement made was the extension of the working distance of the instrument from roughly 2 m to 5 m, which is more or less the minimum useful distance for in-situ high temperature measurements. The complete system has been characterised and validated using the facility (a small-scale industrial furnace capable of simulating industrial conditions in the laboratory) presented in Figure 27b. From the calibration, it is observed that the instrument is somewhat sensitive to the changes of the settings of the optical head (e.g., displacement of the mirrors and the fibre tip, and tilting of the whole optical head assembly) and thus the calibration constant can be different significantly between the previous and the current states of the instrument especially when optical alignment and optical head positioning are performed prior to the temperature measurement. This should be taken into consideration when using the instrument in actual field measurements, where the chance is high that the settings of the optical head can be changed during transport and initial set-up at the site. From the characterization, the determined SNR of the instrument is quite robust (about 15-20 dB). This implies that the prototype instrument can reliably detect the modulated thermal radiances induced by the two laser sources. Taking all of the major uncertainty contributors, the initial measurement uncertainty budget is about 4% at 900 °C ($U(k=2)$). A report describing in detail the characterisation and validation activities regarding the instrument is available. The measurement uncertainty budget is also included in this report. Figure 31 Results of the validation of the active two-colour LART using the small-scale industrial furnace shown in Figure 27b shows the results of the temperature measurement validation.



Figure 30 Active two-colour laser radiation thermometer with the redesigned optical head.

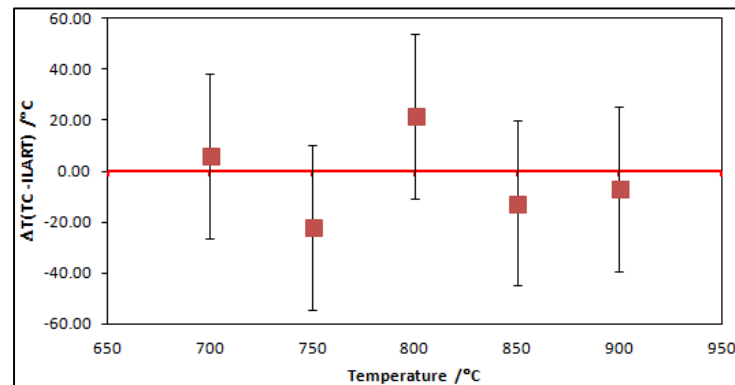


Figure 31 Results of the validation of the active two-colour LART using the small-scale industrial furnace shown in Figure 27b

3.4.6 *Temperature-independent emissivity measurement using the virtual source technique*

The virtual source method for emissivity measurement, proposed and realised by SMU, involves the creation of a so-called “virtual source” by the reflection of the source radiance onto a mirror with known reflectance. This schematic of the experimental realization of the method is illustrated in Figure 32. The radiant flux from the sample consists mainly of two source contributions: the radiation directly coming from the source, and radiation originating from the virtual source (radiation reflected from the mirror). By changing the position of the mirror that creates the virtual source, the resulting signal changes and a typical function for each emissivity value and material is created. The next step in determination of the emissivity is the generation of multiple functions using a mathematic model. The creation of the function depends on multiple variables which are present in the real measurement. By the systematic change of the values of these variables, different mathematical functions are created. Each individual function represents a different emissivity value. By using a mathematical fitting, it is possible to assign the real measured curve (with an unknown emissivity) with a function in which the emissivity is known. What is so attractive with this approach is that we are able to determine precisely the emissivity without the need to perform any temperature measurement of the source. Table 6 shows the results of the emissivity measurements of Inconel 600 sample using the virtual source method. The uncertainty associated with the emissivity measurement is 0.14 ($k=2$). A measurement uncertainty budget is presented in

Table 7. The emissivity values presented in Table 6 were subsequently used to correct for the emissivity for the temperature measurements obtained by the thermal imager with a similar Inconel 600 sample. With this emissivity correction, the resulting temperature reading from the thermal imager agreed very well with the transfer standard thermometer reading ($\Delta T_{\max} = 2\text{ }^{\circ}\text{C}$). The presented emissivity values in Table 6 for Inconel 600 are in good agreement with the literature values.

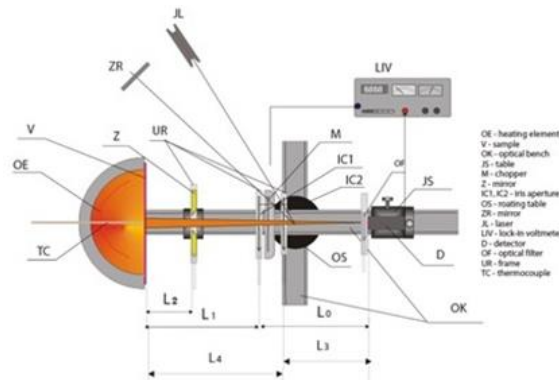


Figure 32 Schematic of the experimental realization of the virtual source method for emissivity measurements.

Table 6 Measured emissivity values for Inconel 600 at different setpoint temperatures using the virtual source method.

Measurement run	$t_s^a = 580\text{ }^{\circ}\text{C}$	$t_s^a = 600\text{ }^{\circ}\text{C}$	$t_s^a = 620\text{ }^{\circ}\text{C}$
	ϵ	ϵ	ϵ
1	0.82	0.85	0.85
2	0.81	0.86	0.92
3	0.86	0.79	0.82
4	0.85	0.85	0.78
5	0.89	0.90	0.75
average	0.85	0.85	0.82
std	0.03	0.04	0.07

^a t_s is the nominal temperature value of the Inconel 600 sample ($^{\circ}\text{C}$)

Table 7 Measured emissivity values for Inconel 600 at different setpoint temperatures using the virtual source method.

Source of uncertainty	Standard Uncertainty	Distribution	Contribution to the standard uncertainty
Emissivity uncertainty (type A)	0.04	Normal (Gaussian)	0.01
Reproducibility	0.03	Uniform	0.02
Sample temperature uncertainty	0.06	Uniform	0.03
Sample temperature distribution	0.10	Uniform	0.06
combined uncertainty U(k=2)			0.14

The objective of this body of work was to develop traceable and accurate techniques for *in situ* surface high temperature measurement. The results obtained in this work directly addressed the various known issues encountered in radiation thermometry, namely emissivity and background reflection, by either reliably accounting for the uncertainty contributions of these factors to the measured temperature or by providing methods to reliably measure these factors such as active two-colour radiation thermometry, traceable gold-cup thermometry and ultraviolet multi-wavelength radiation thermometry.

3.5 *In-situ validation methods for non-contact thermometry to above 2500 °C*

The aim of this objective was devoted to the implementation and testing of self-validation techniques up to 2500 °C with a particular emphasis on the use of these techniques for the correction of window transmission changes while measuring temperature by radiation thermometry.

One of the difficulties at the highest temperatures is to monitor temperature in harsh conditions with possible drift of temperature sensors as thermocouples or pyrometers. Remote measurements through windows using radiation thermometers are also likely to be affected by the progressive obscuration of the window due to deposition of evaporated materials during the use of the furnace for instance.

This work had the aim of proposing innovative solutions for *in-situ* drift and instability correction applied to two industrial applications and to derive a model of temperature correction using high-temperature fixed points to correct for evolving window transmission.

The activities were split in three different parts:

- Development by three partners of robust self-validation cells suitable for industrial use in oxidising and in inert atmospheres;
- Characterisation of the cells to assess their robustness and their reproducibility;
- Implementation in industrial conditions and assessment of their capabilities for varying window transmission correction

3.5.1 *Development and characterisation of the cells*

Two applications in the facilities of the two industrial partners were foreseen in this work: one at CEA for the implementation of graphite-based cells under argon atmosphere, or under vacuum to provide *in-situ* traceability for radiation thermometers and another one at GDF-Suez for the *in-situ* recalibration of type-B thermocouples used for the temperature uniformity assessment in large natural-gas heated glass furnaces.

For both applications, particular cells were designed, characterised and tested in the facilities of both external partners.

3.5.1.1 Graphite cells for inert atmospheres

Three NMIs have joined their efforts to develop rugged cells to be used in the CEA (LMA, mastery of severe accidents Laboratory) induction furnace to enable recalibration of a radiation thermometer through a window. The cells were designed to work in large temperature gradients and heating/cooling rates as compared to gradients and heating/cooling rates usually encountered in a metrology laboratory.

The cells were first characterised in the NMIs after their construction. Having proven robust enough, they were transported to CEA where they were tested together with additional HTFP cells developed by CEA. The induction furnace was cycled from room temperature to temperatures much above the melting temperatures (as much as 400 °C above) with extremely high heating and cooling rates (up to 150 K/min).

Rugged small-sized high-temperature fixed points cells were constructed following the hybrid cell design developed by CNAM [4.1] to serve as in-situ calibration devices in inert atmospheres. The cells, constructed in graphite, were designed to fit the CEA/LPMA furnace. The design was adapted to the particular necessities of induction furnaces, namely large temperature heating/cooling rates and poor temperature uniformities. The outer dimensions were 24 mm in length and 24 mm in diameter. The cavity dimensions were 5 mm in diameter and 15 mm in length which gives a calculated total emissivity of 0.996. The emissivity can be increased to 0.999 by adding a diaphragm of 3 mm diameter at the entrance of the cavity. Figure 33 shows a schematic view of the cell.

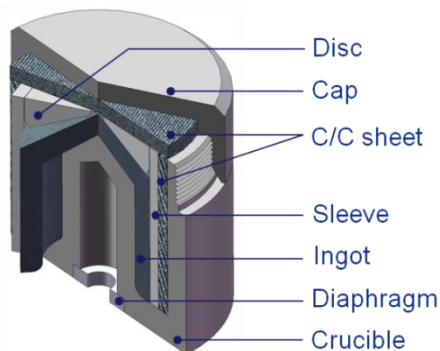


Figure 33 Design of the rugged HiTeMS WP4 HTFP cell adapted from the design for ITS-90 and HTFP cells developed at LNE-Cnam for radiation thermometry.

The cells were filled using the piston method developed by CNAM [4.1, 4.2]. This technique was used successfully in the three NMIs/DIs (NPL, UME and CNAM) to fill the HiTeMS high temperature fixed point cells. While LNE-Cnam and TUBITAK-UME used Vega/VNIIOFI type of high-temperature furnace (HTBB-3200PG and HTBB-3500PG respectively) for the filling, NPL used a modified Chino IR-80 furnace with some modifications to allow LNE-Cnam designed crucibles to be filled.

Several cells at the three high-temperature fixed-points of Co-C (~1324 °C), Ru-C (~1953 °C) and Re-C (~2474 °C) were constructed for this study. TUBITAK UME made five Ru-C cells, NPL made two Re-C cells and CNAM made one Co-C, one Ru-C and one Re-C cells. Table 8 summarises the details about the cells.

Table 8 Summary of the cells constructed at NPL, TUBITAK UME and CNAM

Fixed point, identification of the cells	Nominal purity of the metals (%)	Mass of the ingot (g)
Ru-C-01 (UME)	99.9	13.65
Ru-C-02 (UME)	99.9	13.84
Ru-C-03 (UME)	99.9	16.12
Ru-C-04 (UME)	99.9	16.40

Ru-C-05 (UME)	99.9	14.38
HRe#1 (NPL)	99.999	30.2
HRe#2 (NPL)	99.999	30.2
Co-C HCo (CNAM)	99.998	10.47
Ru-C HRu (CNAM)	99.998	11.39
Re-C HRe (CNAM)	99.997	24.53

At the end of the filling process the cells were submitted to several melt/freeze cycles by each partner to assess the metrological characteristics of the plateaux. The objective of these multiple melt and freeze cycles was to assess the robustness of the cell under particularly tough conditions: heating and cooling rates were set at the maximum levels achievable in the furnaces (in case of the Chino IR-80 furnace reaching about 60 °C/min and -50 °C/min, respectively). The cells were also overheated in the molten state by several hundreds of degrees.

In most cases, the repeatability of the melting temperatures was worst and the melting ranges larger than those obtained with the conventional cell design. This is however understandable due to the small dimensions of the cells, the small amount of metal used and the lower purity level of the metals used for filling the cells. However for most industrial applications the performance was more than adequate.

Figure 34 and Figure 35 show typical results of thermal cycling of the cells, for instance for the Co-C point for which the risk of breakage was considered as the highest among the three fixed points due to differential expansion factors.

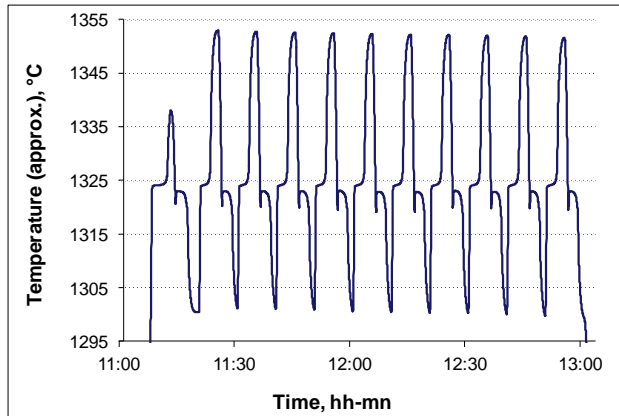


Figure 34 Cycling of the Co-C cell allowing to assess the repeatability of the melting temperature (determined at the point of inflection of the melting plateau) to better than 50 mK.

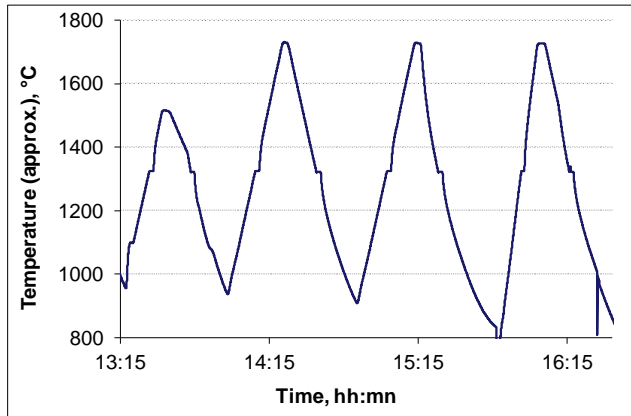


Figure 35 The cell was heated to 1700 °C, approximately 400 °C above the melting temp

The main output of these characterisation tests was that all the cells developed at NPL, CNAM and TUBITAK-UME, were successfully qualified for use in the facilities of CEA, where they have to withstand more difficult conditions with larger heating and cooling rates, larger temperature gradient and more substantial overheating. Further details about the cells and the characterisation results can be found in [4.3, 4.4].

3.5.1.2 Alumina cells for oxidising atmospheres

For the needs of the in-situ recalibration (or drift compensation) of a Type B thermocouple devoted to the temperature uniformity determination in a 500 kW furnace of GDF-Suez, two Ni cells were constructed in CNAM (Figure 36 and Figure 37). The requirements for these cells were the possibility of running them in oxidising atmospheres, having dimensions which could fit the thermocouples used and showing a phase transition temperature slightly below 1500 °C. Therefore alumina was chosen as the crucible material and Nickel as the fixed point material with an expected melting temperature around 1450 °C.

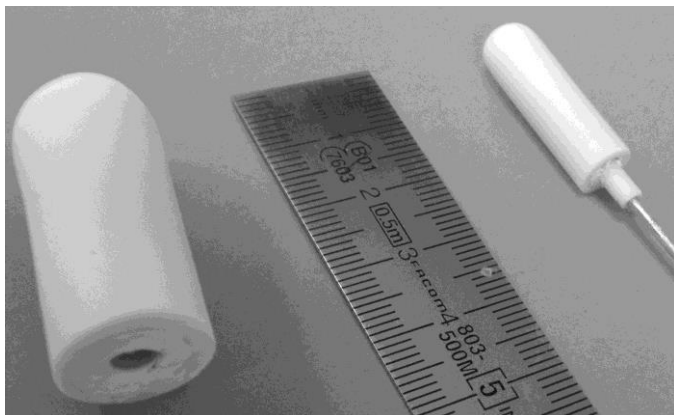


Figure 36 Ni cells with alumina crucibles developed for oxidising atmospheres.



Figure 37 The large cell as it was installed on the GDF thermocouple during the in-situ tests.

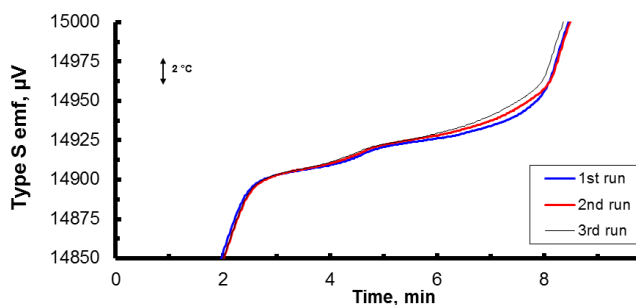


Figure 38 Melting plateaus of the Ni cell (in alumina crucible) observed during the characterisation of the cell at CNAM.

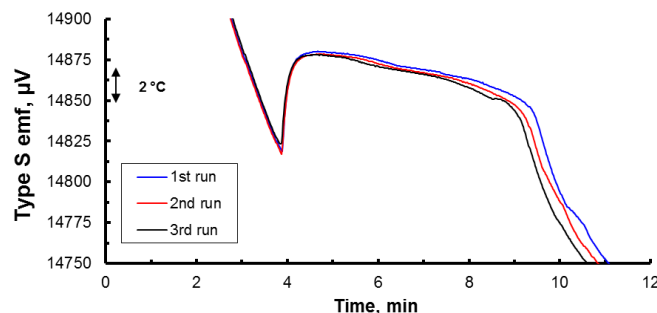


Figure 39 Freezing plateaus of the Ni cell (in alumina crucible) observed during the characterisation of the cell at CNAM.

The cells were first tested to check the quality of the plateaux and the repeatability of the measured phase transition temperatures. Figure 38 and Figure 39 show the plateau shapes obtained with the largest cell in Figure 36. This cell is 3.5 cm in length, 10 mm in diameter and has a thermocouple well of 4 mm in diameter. It contains 12 g of a 99.95 % purity Nickel.

The repeatability of the melting temperatures determined as the point of inflection of the melting plateau was within 0.5 K. The Freezing temperature showed the same level of repeatability.

3.5.2 In-situ test results

3.5.2.1 Measurements at CEA

Six out of ten cells developed in this work package were transported to CEA and studied in the VITI induction furnace (Figure 40 and Figure 41). The objective was to assess the robustness of the cells and their use for traceability transfer and correction of window transmission [4.4].



Figure 40 Installation of the HTFP cells in the CEA VITI induction furnace

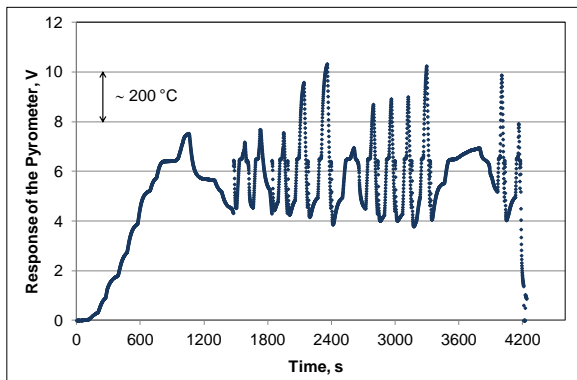


Figure 41 The results of the cycling of the NPL Re-C cell

The main output of these tests was that all the cells produced in the frame of this work which have been implemented in the VITI furnace, withstood without damage large heating and cooling ramps of up to 150 K/min. The plateaux could be observed using a radiation thermometer through a window allowing an in-situ recalibration of the furnace temperature controller. The cycling of the cells around the corresponding melting temperatures was performed. Figure 41 shows a typical pattern of cycling of Re-C cells during which multiple plateaux were recorded with very large heating/cooling rates and overheating which could reach 400-500 °C. In all cases, the plateaux were still exploitable.

These measurements through windows allowed the testing of window transmittance correction. Even in case of misknowledge of the spectral characteristics of the pyrometer (central wavelength and bandwidth) it is possible to use the pyrometer signal correction at one or two fixed points (with some basic hypotheses) to derive an estimate of the window transmittance and the temperature measured through the window. Further details can be found in [4.5, 4.6].

3.5.2.2 Measurements at GDF-Suez

The large Ni cell constructed and characterised at CNAM was installed on a Type-B thermocouple (Figure 36 and Figure 37) and tested in the 500 kW natural gas heated furnace.

Figure 42 shows the results of the first tests in the high-temperature natural-gas furnace of GDF. The cycling of the cell in this furnace was performed during a whole day. The melting and freezing plateaux could be observed though the freezing was less visible.

The cell proved efficient in supplying a repeatable (~1K) reference temperature which allowed the in-situ drift compensation to be effectively confirmed.

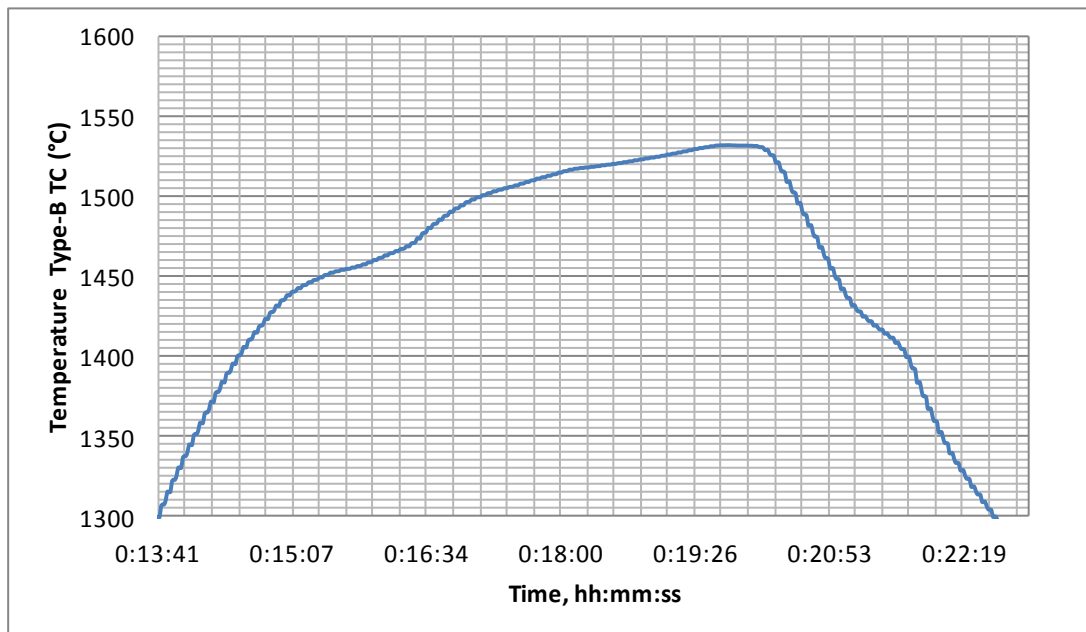


Figure 42 melting-freezing plateau of the Ni cell measured in the GDF furnace using a type B thermocouple

3.5.3 Conclusions

This work enabled a thorough and complete analysis of the capabilities of high-temperature fixed points to be adapted to an industrial use and yet to be able to act as a means for traceability and temperature monitoring in harsh measuring conditions.

The HTFP cells developed in this project and constructed at three different NMIs with the same cell design and the same filling method have been characterised to assess their reproducibility and their robustness before being transported and tested in the CEA facilities. These cells were operated under steep heating and cooling rates and large melting steps causing overheating of several hundreds of degrees in order to simulate extreme in-process working conditions. In all cases, the cells performed as expected and proved robust and reliable. Furthermore a Nickel cell was also constructed and tested at CNAM before being tested and validated in the facilities of GDF as a means of drift compensation for a thermocouple.

The objective of this body of work was to demonstrate *in situ* validation methods for non-contact thermometry to above 2500 °C.

The results obtained have shown that the use of high-temperature fixed points as *in-situ* references is possible even in the harsh conditions imposed by induction heating and the presence of a continuously obscuring window. Algorithms allowing the correction of evolving window transmission have been developed and applied successfully. Moreover, the technique of self-calibrating thermocouple in oxidising atmosphere was tested and validated in industrial harsh conditions, in a flame-heated glass furnace. This work has reached all the technical objectives and went even beyond.

3.6 *In-situ* traceable temperature measurements for exotic thermal processing methods

Laser surface heat treatment for steel or cast iron parts with high-power diode lasers has been established in industrial mass production during the last 15 years. Due to the high power density of the laser heat sources and the high processing temperatures, which are often desired to be close to the melting temperature of the materials, a precise temperature measurement and control is essential for a reproducible parts quality. For the

successful heat treatment of special high-alloyed steel grades or gray cast iron surfaces, the process temperature needs to be controlled within a band of only a few Kelvin at a temperature of around 1200 °C. A too high temperature can lead to a part melting and a temperature too low will result in a lower surface hardness and a reduced penetration depths.

One key problem of the temperature measurement by laser and radiation thermometer is the nonlinear signal damping by the laser optics and contamination and wear of optical components during their lifetime, e.g. by processing fumes. On-site calibration is needed because the temperature measurement devices are mechanically and electrically integrated into complex machine systems.

A mobile induction-heated fixed-point device was developed to allow for a calibration in the temperature range 1000–1500 °C onsite and evaluated at industrial set-ups.

In a first step, the different variants of temperature measurement systems, typically used in industrial laser heat treatment, were investigated by FhG to define the requirements for the device. The arrangement of system components and processing parameters of the induction-heated fixed-point device were subsequently optimised by a computer simulation with FEM and FDM.

Based on the results, a prototype of an induction-heated fixed-point device was designed and manufactured by PTB.

The device consists of a water-cooled and vacuum-sealed housing with ports for connection to a vacuum pump, shielding gas supply, a specially designed lead-through of the induction coils and optical windows. All equipment can be installed in a rack for good system mobility. For safety reasons, all important system parameters such as shielding gas flow, water flow and temperature, and residual oxygen content are measured and observed. The fixed point cell is covered in a graphite felt and held in a ceramic container placed in the induction coil.

In this device fixed-point cells of Cu, Fe-C, Co-C were manufactured at PTB. The fixed-point cells cover the temperature range from 1084.6 °C to 1323 °C. To take account of the different measurement spot sizes two cell designs with 3 mm and 5 mm diameter cavity diameter were developed.

Different factors influencing the accuracy and reproducibility of the fixed-point plateau temperatures were experimentally investigated, i.e. the position of the fixed-point cell relative to the induction coil, the arrangement of the thermal insulation, the parameters for overheating and undercooling of the cell to initiate the melt and freeze of the metal alloy and variations in the induction frequency. As the fixed-point material is in part directly heated by induction, for repositioning the cell a change in melting temperature of up to ± 0.5 K was observed.

In a next step the fixed point device was used to evaluate the absolute accuracy of the temperature measurement systems in industrial laser hardening set-ups at Fraunhofer IWS and Alotec Dresden GmbH, Germany. Large deviations of up to several 10 K were found in these set-ups, which originate from the large uncertainties of the initial onsite calibration and from continuous wear and contamination of the optical set-ups from process fumes and mechanical damages of the optical surfaces.

Besides a validated understanding of the measurement accuracy of the radiation thermometer, a precise knowledge of the spectral emissivity of the work piece is necessary for a reliable temperature measurement.

As cost-efficient and mobile measuring devices are currently not available, the direct and accurate emissivity measurement is often not achievable. Consequently, the values of an emissivity optimization can often be only roughly estimated with the help of tables. Quite often, this procedure makes the measuring result uncertain; especially since variations, caused by oxidation, might occur during the running process.

For this reason, the influence of laser hardening and heat treatment of typical steels and cast iron was investigated in the temperature range up to 1300 °C by ZAE, PTB and SMU. The investigated materials were steels 1.1730, 1.2344, 1.2379 and 1.4548 and cast iron GGG-70.

For all materials and in the spectral range between 1 and 10 micron the spectral emissivity was found to increase with the surface roughness (from polished to a turned to a sandblasted surface in increasing order). Heat treatment under oxidising conditions will result in oxide layer growth on the parts surface. Towards longer wavelength (between 5 and 10 microns) the growing oxide layer was observed to change the spectral emissivity drastically, i.e. from around 0.2 to 0.7, whereas for smaller wavelength (<1 micron) after an initial step change in emissivity with the build-up of the oxide layer from around 0.5 to 0.8 the spectral emissivity was observed to change only slightly.

This objective was to demonstrate in situ traceable temperature measurements for exotic thermal processing methods such as laser hardening.

Essential for an accurate non-contact temperature measurement is an understanding of the materials emissivity. For this reason the spectral emissivities for samples of typical work steels with the different surface preparations were investigated. A traceable temperature measurement in laser hardening requires the measurement system to be calibrated in regular intervals. Up to now a re-calibration of the measurement system has been difficult as the radiation thermometer is part of the complex laser optical unit and reliable and compact reference artefacts were not available for an onsite calibration.

By developing a mobile, induction-heated fixed-point device such a temperature reference artifact is now available for the temperature range between 1084.6 °C and 1323 °C. This device was successfully tested at several industrial sites. The results above have directly contributed to achieving this objective.

4 Actual and potential impact

The lifetime and drift of thermocouples were not at all well known before the start of this project; in addition manufacturers of such sensors had their own procedures and approaches to testing their products. By the end of this research we had:

- Developed capability for the reliable drift and lifetime characterisation of thermocouples at high temperatures – accessible to manufacturers of thermocouples.
- Developed new knowledge in particular on the drift characteristics of thermocouples and started to understand how drift correction might be implemented due to relatively predictable drift with exposure time at particular temperatures. If results are confirmed this would lead to improved process efficiency and also reduced sensor exchange.
- Developed and published a EURAMET Guide on Lifetime and Drift/Stability Assessment of Industrial Thermocouples (No. 2 5/2015) to standardise the lifetime and drift assessment of thermocouples. This is freely available from the Euramet website and can be used by any manufacturer of high temperature thermocouples and in fact is already in use by a number of the unfunded partner/collaborator institutes with HiTeMs.

There are many different combinations of wire alloys that could be used to produce new thermocouples, some of which could potentially convey significant advantage to industry in terms of improved drift performance or higher temperature use. However they are not used because there was, until this project was performed, no agreed method, or qualified facilities, for characterising such sensors temperature versus output with low uncertainties. By the end of the HiTeMS project this unsatisfactory situation had been resolved and we had:

- Developed an EU distributed facility for determining the reference function of novel thermocouple types to 2000 °C with low uncertainties. This was by two different technical methods which in combination facilitated low uncertainties for the reference function. This facility is now available to EU sensor manufacturers who wish to determine the reference function of any newly developed thermocouples to high temperatures.
- Demonstrated the performance of the facility thorough determining the reference junction of the so-called “Land-Jewel” Pt/Rh alloy thermocouple, and in the process discovered a problem with its published reference function.
- In addition this facility will be used in the EMPIR project Enhanced Process control through improved temperature measurement “EMPRESS” to identify the optimum alloy composition for Pt/Rh thermocouples in an effort to maximise temperature level, and minimise drift rate and uncertainty of a new thermocouple type.

Contact temperature sensors drift in use, and usually in unpredictable amounts and ways at high temperatures. This can be caused by contamination from the process, it can be caused by impurities in the thermocouple wires or insulators, or it can be caused by inhomogeneity growth within the wires themselves. This causes significant problems for manufacturers who rely on such sensors to control their processes at particular temperatures to ensure that uniform high quality products are produced at minimum cost and waste. Here the HiTeMS consortium sought to develop a number of approaches to determine or even to mitigate temperature sensor drift *in-situ*. By the end of the project new approaches to *in-situ* sensor drift determination had been demonstrated. In particular we had:

- Developed and demonstrated at least two approaches to *in-situ* validation of thermocouples by incorporating miniature fixed points within the measurement junction of the thermocouple. Some of the results of this particular research are feeding directly into the EMPIR “EMPRESS” project where self-validating sensors, based on this approach, will be modified and packaged so as to be tested in real industrial environments such as heat treatment of aerospace components.
- Developed a combined primary thermometer electrical noise sensor and a noble metal thermocouple. This has the potential advantage of the speed of a thermocouple coupled with the reliability of a primary effectively driftless approach. The sensor and whole approach had been taken to proof of concept stage by the end of the project, though requires further development before it can be tested in an industrial setting.

Non-contact thermometry: The same outcomes as contact thermometry, new knowledge, new approaches and new facilities developed through the research performed in HiTeMS. There were two main outcomes of the research performed concerning improving non-contact thermometry. These are described below:

- 1) The determination of reliable and traceable surface temperatures by non-contact thermometry is a serious issue with non-contact thermometry. In many processes uncertainty in measurement is poorly characterised and the effect of reflected thermal radiation, surface emissivity and target size is poorly understood. This leads to relatively coarse process control which in turn leads to non-optimum energy use, higher carbon emissions and potentially higher scrap rates. These are very large problems for which we could not hope to provide comprehensive solutions within the budget or timeframe of the project, however there were some notable progress in some areas, in particular:
 - New capability was established for determining the effect of reflected thermal radiation on gold cup thermometers (widely used in industry). This facility enables for the first time uncertainties in the approach to be characterised both for sloping and curved surfaces and for varying surface emissivity.
 - A new facility was established for quantifying the uncertainty due to the size of source characteristics of industrial non-contact thermometers.
 - New capabilities to determine surface emissivity were established increasing capacity for such measurement within the EU.
 - All of the above will contribute to improving the practice of non-contact thermometry in an industrial setting and all the facilities are available for use by industry.
- 2) A second serious issue besetting radiation thermometry is that of variable and unquantified transmission of the path between the non-contact thermometer and the object being measured. This can lead to industrialists running their processes at significantly higher temperatures than are required which in turn uses more energy than required, lead to a reduction in product quality and increase in scrapage. For e.g. in laser heat treatment the temperature window for effective thermal treatment is very narrow – too high leads to melting, too low leads to ineffective treatment. The research performed as part of HiTeMS demonstrated the potential for big improvements in that economically important sector for the EU. In particular;
 - A completely novel approach to determining window transmission *in-situ* was developed AND trialled in two independent industrial settings, namely nuclear power safety research and laser heat treatment.

- Robust high temperature fixed points of known temperature were incorporated within the process and their reference temperature and radiance used to determine the transmission of progressively contaminating windows. This allowed corrections to be applied for the window transmission and it was demonstrated that, in particular for the heat treatment application, that significant process improvements could be gained if *in-situ* calibration of control non-contact thermometers, through the methods developed in this project, were to be implemented.
- An emissivity database of materials that undergo heat treatment was established. This, in combination with the *in-situ* transmission corrections, allowed, for the first time, truly traceable, low uncertainty temperature measurements to be performed in laser heat treatment.

The above give the highlights of the achievements of HiTeMs and the new and improved measurements that are now possible because of the research performed in that project. A summary paper has been written on the project and submitted to the journal *Measurement*¹, this has been accepted for publication and will appear later in 2015. That paper summarises the key technical achievements of the HiTeMs project, and gives references to many of the papers produced during the project. Finally to ensure the maximum dissemination of the results a presentation summarising the achievements of HiTeMs will be given at the forthcoming International Congress of Metrology in Paris in September 2015.

The impact of our successful achievement of this project's objectives may be summarised as follows:

1. Rigorous, traceable techniques to enable lifetime testing and stability evaluation of contact temperature sensors above 1000 °C

A robust, reliable and traceable method for determining the lifetime and drift of thermocouples has been established. This process has been formalised, published and freely available as a EURAMET Guide on Lifetime and Drift/Stability Assessment of Industrial Thermocouples (No. 2 5/2015).

As part of this project a number of NMIs developed capability for the reliable drift and lifetime characterisation of thermocouples at high temperatures, these are now accessible to manufacturers of thermocouples.

New knowledge on the drift characteristics of thermocouples was determined during this project. Understanding the performance limitations of such sensors is important to suppliers of such sensors and for anyone who may go on to use them in industrial process control.

2: Self-validating contact temperature sensors for use from 1000 °C to above 2000 °C

The extensive material compatibility studies surpass the specific application of the high temperature miniature fixed points together with MIMS thermocouples by far. These studies provided general technical expertise in common high temperature applications for users and manufacturers in production process to improve process efficiency by choosing more suitable and reliable materials.

The use of integrated miniature fixed points as self-validating devices offer a cost-efficient method to perform a one-point validation of a thermometer by minimal material consumption and acceptable accuracy. Furthermore, the investigation of different designs of self-validating fixed-point devices and the results obtained allow the users to favour or to exclude special designs for their applications. Four pure metals (Au, Ni, Pd, and Pt) with different melting temperatures in the temperature range between 1064 °C and 1769 °C in oxidizing atmospheres and two metal-carbon eutectics (Pt-C and Ru-C) for use in inert atmospheres up to 1953 °C were investigated as fixed-point materials. Especially the successful application of the two metal-carbon cells promise the use of other metal-carbon fixed points to extend the temperature range for self-validating methods in inert atmospheres.

The results obtained by using combined thermocouple-noise temperature sensors initiated interest of a European steel producer to have reference measurements performed by using such a combined sensor at temperatures of about 1250 °C.

¹ Machin, G., Anhalt, K., Battuello, M., Bourson, F., Dekker, P., Diril, A., Edler, F., Elliott, C., Girard, F., Greenen, A., Křazovická, L., Lowe, D., Pavlásek, P., Pearce, J., Sadli, M., Strnad, R., Seifert, M., Vuelban E. M., "The research outcomes of the European Metrology Research Programme Project: HiTeMS – High Temperature Measurement Solutions for Industry", *Accepted for publication in Measurement 2015*

3: A methodology for the rigorous determination of 'reference functions' for non-standard thermocouple types

The principal means of dissemination have been via a) peer-reviewed publications, b) direct discussion with stakeholders including major thermocouple manufacturers, and c) discussion with standards bodies, in particular IEC. The main achievement of WP6 is the establishment of a pan-European facility for rapid, straightforward determination of the reference function (voltage versus temperature relationship) for non-standard and novel thermocouples.

This is an important facility, because as process temperature control requirements become ever more demanding, the demands on the stability of thermocouples exceed current capabilities, and there is growing interest in new thermocouple types. In particular, the optimisation and refinement of existing high temperature thermocouples such as those based on Pt-Rh alloys really requires access to a rapid technique for characterising those thermocouples so that they can be used. Other applications include new thermocouples for harsh environments such as those with low neutron capture cross-sections for the nuclear industry, and more exotic graphite-based thermocouples.

Developments from this objective are already feeding into new project proposals: the European facility is an important part of a new proposal submitted to the EMPIR 2014 Industry call as part of an activity to find an optimum, ultra-stable Pt-Rh thermocouple for use to 1800 °C. Furthermore, the deficiencies of the Pt-40%Rh versus Pt-20%Rh thermocouple identified as part of the WP6 research will lead to further work to better characterise this, with the aim of possibly refining the ASTM E1751 standard and also incorporating this thermocouple type in an IEC standard such as IEC 60584. This will be a priority activity in future research and development because the conventional thermocouple types R, S, and B can only really be used up to about 1500 °C reliably; above this temperature, drift becomes a significant problem. Meanwhile several industries need to use this type of thermocouple to 1800 °C (e.g. casting, sintering of ceramics such as nuclear fuels, manufacture of silicon-based products for e.g. photovoltaics). The outputs will play a major part in these developments.

4: Traceable and accurate radiation measurement techniques for *in-situ* surface high temperature measurements above 1000 °C

Metrological impact:

Substantial reduction of the measurement uncertainties for temperature has been demonstrated by INRIM with their developed and validated prototype UV-multiwavelength thermometer. The conclusion drawn from the investigation done by VSL on the scanning-slit method for determining size-of-source effects (SSE) is valuable in implementing this method, as alternative to the direct and indirect methods, for fast and robust calibration of radiation thermometers with regards to SSE uncertainty contribution. Determining the contribution of the surface geometries (sloped and curved surfaces) to the overall measurement uncertainties with gold-cup radiation thermometers (GCRT) provides further significant improvement to the reduction of uncertainties in industrial temperature measurements. The outcome from the development activity on the active two-colour laser-based radiation thermometer also lead to a better measurement uncertainty budget for the instrument (about 4% at 900 °C and above), which is for industrial measurement applications an improvement of at least a factor of 2.

Dissemination activities (Scientific Publications, Conferences):

The results of the research and development activities undertaken within this project have been presented in two major conferences (in total, 3 oral presentations and 1 poster presentation) and published in 2 peer-reviewed articles in scientific journals. Furthermore, three manuscripts were submitted to peer-reviewed journals and awaiting final approval. A general overview of the technical results was also presented during the project stakeholders workshop held in Paris last May 2014.

Early and Potential Impact:

Based on the insights learned from the developed prototype, to prove the concept of a UV-multiwavelength thermometer, there is huge potential for implementing this technique (using a compact PDA spectrometer) in real industrial measurement applications. For the emissivity determination using the virtual source approach,

SMU plans to implement this into their standard metrological service for industry. The better characterisation of gold cup pyrometers by the simulated industrial environment at VSL will, for the first time, enable users of such devices to quantify uncertainty components for sloping and curved surfaces. Furthermore, the use of the active two-colour laser radiation thermometer in industrial temperature measurements will provide an uncertainty much better than what are typically encountered with other techniques.

5: *In-situ* validation methods for non-contact thermometry to 2500 °C, including demonstrating novel drift correcting techniques

The graphite cells developed in this objective will have a double use: as *in-situ* reference points for inert atmospheres but also as travelling artefacts for comparisons (case of the CCT comparison in radiation thermometry above Ag point).

Two workshops were held (Metrologie 2013 and at the final meeting of HiTeMS, both in Paris) to present the achievements of the project.

A paper was accepted and is under final adjustment for a trade journal (Essais Mesures Contrôles – a French journal well spread in Industry) to present the application of self-validation techniques in CEA and GDF.

6: A demonstration of *in-situ* traceable temperature measurements for exotic thermal processing methods such as laser hardening

The technological developments for an improved temperature measurement in laser hardening have been presented and discussed with end users at various occasions (e.g. exhibition of the fixed-point furnace at the fair Hannover fair in 2012 and 2013, and exhibition of fixed-point cells at LASYS fair for laser material treatment 2012). With FhG a direct stakeholder was involved in the development and evaluation of the fixed point furnace, the REG was trained at PTB and NPL in precision radiation thermometry and manufacture of fixed points. As the REG will continue to work for FhG the outcome of the WP will also in future lead to additional uptakes, as FhG will continue to develop, manufacture and implement laser hardening machines induction for industrial customers (e.g. automotive and energy conversion – steam turbines). Already FhG is planning to develop a miniaturised fixed point device for use on the sites of FhG and their customers during maintenance and service of existing set-ups.

FhG and Alotec a job shop laser hardener in Dresden, Germany have successfully tested the device and found deviation in temperature measurement of up to several 10 K with the currently used calibration, while the novel approach here allows a measurement uncertainty of 1 – 2 K.

5 Website address

<http://projects.npl.co.uk/hitems/>

6 List of publications (published on date of submission)

C. Parga, C. Journeau, A. Tokuhiko, "Development of metal-carbon eutectic cells for application as high temperature reference points in nuclear reactor severe accident tests: Results on the Fe-C, Co-C, Ti-C and Ru-C alloys' melting/freezing transformation temperature under electromagnetic induction heating", High Temperatures-High Pressures, November 2012, Volume 41, Number 6, 2012, p. 423-448

M. Rydzek, T. Stark, M. Arduini-Schuster, J. Manara, "Newly Designed Apparatus for Measuring the Angular Dependent Surface Emittance in a Wide Wavelength Range and at Elevated Temperatures up to 1400° C", Journal of Physics: Conference Series, December 2012, 2012 J. Phys.: Conf. Ser. 395 012152.

M. Seifert, K. Anhalt, C. Baltruschat, S. Bonss, B. Brenner, "Precise temperature calibration for laser heat treatment", *J. Sens. Sens. Syst.*, 2014, pp. 47-54

F. Girard, M. Battuello and M. Florio "Multi-Wavelength Thermometry at High-Temperature: Why it is Advantageous to Work in the Ultra-Violet", *Int J Thermophys* (2014) 35:1401–1413 DOI 10.1007/s10765-014-1678-1

References

- [3.1] White D R, et al, 1996, The status of Johnson noise thermometry, *Metrologia*, **33**, 325-335
- [3.2] Brixy H, Hecker R, Höwener, and Rittinghaus K F, 1982, Applications of noise thermometry in industry under plant conditions, *Temperature, its Measurement and Control in Science and Industry*, Vol. 5 (Ed. by Schooley) New York, , AIP, 1225-1237
- [3.3] C. J. Elliot, M. J. Large, J. V. Pearce, G. Machin, Compatibility of Materials for Use at High Temperatures with W-Re Thermocouples, *Int J Thermophys*, (2014) **35**: 1202-1214
- [3.4] F. Edler, Miniature fixed points at the melting point of palladium, *Proc. TEMPMEKO 1996* (Ed. P Marcarino, Levrotto & Bella, Torino), 1997, pp.183-188
- [3.5] S. Mokdad, G. Failleau, T. Deuzé, S. Briaudeau, O. Kozlova and M. Sadli, A self-validation method for high-temperature thermocouples under oxidising atmospheres, *TEMPMEKO 2013 – under review at IJOT*
- [3.6] Edler F, Kühne M, and Tegeler E, 2004 Noise temperature measurements for the determination of the thermodynamic temperature of the melting point of palladium, *Metrologia* **41**, 47-55
- [4.1] F. Bourson, S. Briaudeau, B. Rougié, M. Sadli, "Developments around the Co-C eutectic point at LNE-INM/Cnam", *Presented at Tempbeijing 2008*, Beijing, 20-23 October 2008 (paper 16. CD-Rom)
- [4.2] M. Sadli, O. Pehlivan, F. Bourson, A. Diril, K. Ozcan, *Int J Thermophys*, **30**, 36–46 (2009).
- [4.3] M. Sadli, T. Bellin-Croyat, F. Bourson, T. Deuzé, A. Diril, G. Failleau, C. Journeau, D. Lowe, S. Mokdad, C. Parga, N. Richard " High-Temperature Fixed Points for Industrial Applications" *presented at TEMPMEKO 2013*.
- [4.4] C. Parga, F. Bourson, M. Sadli, C. Journeau "Cellules à points fixes de température pour la recherche appliquée" In Proceedings of Congrès de la Société Française de Thermique SFT-2013, Gérardmer, 28-31 May 2013.
- [4.5] D. Lowe, F. Bourson, C. Journeau, G. Machin, C. Parga, M. Sadli, "Correction for window transmission in radiation thermometry using high temperature fixed points", In Proceedings of the International Metrology Conference "Métrologie 2013", Paris, 7-10 October 2013.
- [4.6] D. Lowe, G. Machin, M. Sadli "Correction of temperature errors due to the unknown effect of window transmission on ratio pyrometers using an in-situ calibration standard" to be published in *Measurement*.
- [6.1] P.A. Kinzie, Thermocouple Temperature Measurement, John Wiley & Sons, Inc. (1973) ISBN 0-471-48080-0
- [6.2] F. Edler and P. Ederer, Thermoelectric homogeneity and stability of platinum-rhodium alloyed thermoelements of different compositions, *AIP Conf. Proc.* 1552, 532 (2013)
- [6.3] A. Ulanovskiy, V. Medvedev, S. Nenashev, A. Sild Yu, M. Matveyev, A. Pokhodun, P. Oleynikov, *Int. J. Thermophys.* 31(8-9), 1573-1582 (2010)
- [6.4] H. Ogura, M. Izuchi, J. Tamba, Stability of Tungsten Rhenium thermocouples in the range from 0 °C to 1500 °C, *Int. J. Thermophys.* 32, 2420-2435 (2011)
- [6.5] H. Brixy, "Noise Thermometry", in *Experimental Techniques of Physics*, Managing editors E. Klose, Wilhelmi Vol 40 (1994) no. 1 ISSN 0014-4924 (Heldermann Verlag)
- [6.6] B.E. Walker, C.T. Ewing, R.R. Miller, *Rev. Sci. Instr.* 33(1), 1029 (1962)
- [6.7] B.E. Walker, C.T. Ewing, R.R. Miller, *Rev. Sci. Instr.* 34(12), 1456 (1963)

- [6.8] A.A. Rudnitskii and I.I. Tyurin, *J. Inorg. Chem. (USSR)* 1, 207 (1956) (English translation)
- [6.9] C.B. Alcock and G.W. Hooper, "Thermodynamics of the gaseous oxides of the platinum-group metals", in *Proc. R. Soc. Lond. A* 254, 551-561 (1960)
- [6.10] J.C. Chaston, The oxidation of the platinum metals, *Platinum Metals Rev.*, 19(4), 135 (1975)
- [6.11] R.C. Jewell, E.G. Knowles, T. Land, *Metal Ind. London* 87, 217 (1955)
- [6.12] F.R. Caldwell, *J. Res. Natl. Bur. Std.* 10, 373 (1933)
- [6.13] E.D. Zysk, *Engelhard Ind. Tech. Bull.* 5, 69 (1964)
- [6.14] P.D.S. St. Pierre, *Bull. Am. Ceram. Soc.* 39, 264 (1960)
- [6.15] R.E. Bedford, *Reference Tables for Platinum-40% Rhodium / Platinum-20% Rhodium Thermocouples*, *Rev. Sci. Instrum.* 36(11), 1571-1580 (1965)
- [6.16] ASTM E 1751 – 09: "Standard Guide for Temperature Electromotive Force (emf) Tables for Non-Letter Designated Thermocouple Combinations", ASTM, 100 Barr Harbor Drive, West Conshohocken, PA 19428-2959, USA
- [6.17] H. Preston-Thomas, The International Temperature Scale of 1990 (ITS-90), *Metrologia* 27, 3-10 (1990); see also erratum in *Metrologia* 27, 107 (1990)
- [6.18] Y. Yamada, H. Sakate, F. Sakuma, A Ono, High-temperature fixed points in the range 1150 ° to 2500 °C using metal-carbon eutectics, *Metrologia* 38, 213-219 (2001)
- [6.19] E.R. Woolliams, G. Machin, D. Lowe, R. Winkler, Metal (carbide)-carbon eutectics for thermometry and radiometry: a review of the first seven years, *Metrologia* 43, R11-25 (2006)
- [6.20] F. Edler and A.C. Baratto, A cobalt-carbon fixed point for the calibration of contact thermometers at temperatures above 1100 °C, *Metrologia* 42, 201-207 (2005)
- [6.21] J.V. Pearce, H. Ogura, M. Izuchi, G. Machin, Evaluation of the Pd-C eutectic fixed point and the Pt/Pd thermocouple, *Metrologia* 46 (2009) 473-479
- [6.22] H. Ogura, M. Izuchi, M. Arai, Evaluation of cobalt-carbon and palladium-carbon eutectic fixed point cells for thermocouple calibration, *Int. J. Thermophys.* 29, 210-221 (2008)
- [6.23] F.H. Schofield, *Proc. Roy. Soc. A.*, 146 792 (1934)
- [6.24] W.F. Roeser, F.R. Caldwell, H.T. Wensel, *Bur. Std. J. Res.* 6 1119 (1931)
- [6.25] F. Hoffmann, C.Z. Tingwaldt, *Physik*, 34, 434, (1934)
- [6.26] R.E. Bedford, G. Bonnier, H. Maas, and F. Pavese, Recommended values of temperature on the International Temperature Scale of 1990 for a selected set of secondary reference points, *Metrologia* 1996, 33, 133-154
- [6.27] G. Machin, K. Anhalt, F. Edler, J.V. Pearce, M. Sadli, R. Strnad, E.M. Vuelban, HiTeMS: A project to solve high temperature measurement problems in industry, *AIP Conference Proceedings* 1552, 958 (2013)
- [6.28] M. J. Martin, M. Zarco, D del Campo. *Int. J. Thermoph.* 32, 383-395 (2011)
- [6.29] F. Edler, M. Anagnostou, J. Bojkowski, S. Gaita, C. Garcia, E. Grudniewicz, F. Helgesen, J. Ivarsson, A. Pauza, p. Rosenkrantz, M. Smid, T. Weckstrom, D. Zvizdic, Intercomparison of Copper Fixed-Point Cells by Using Pt/Pd Thermocouples, *Int J Thermophys* (2008) 29(1), 171–180
- [6.30] C. García Izquierdo, M. J. Martín, J. M. Mantilla, D. del Campo. Assignment of t90 temperature to a vertical Co-C cell for thermocouple calibration, *Int. J. Thermophys.* (to appear)
- [6.31] F. Jahan and M. Ballico, A study of the temperature dependence of inhomogeneity in platinum-based thermocouples, in *Temperature: Its Measurement and Control in Science and Industry* vol 7, ed. D.C. Ripple (New York: AIP) pp. 469-474
- [6.33] F. Edler, R. Morice, H. Ogura, J.V. Pearce, Investigation of Co-C cells for improved thermocouple calibration, *Metrologia* 47(1), 90-95 (2010)

- [6.34] J.V. Pearce, F. Edler, C.J. Elliott, G. Failleau, R. Morice, H. Ogura, Investigation of Pd-C cells to improve thermocouple calibration, *Metrologia* 48, 375-381 (2011)
- [6.35] H. Ogura, T. Deuzé, R. Morice, J.O. Favreau, *Int J Thermophys* 32 :7-8, pp 1811-1823 (2011)
- [6.36] R. Morice, H. Ogura, J.O. Favreau, T. Deuzé, P. Ridoux, *Acta Metrologica Sinica* 29, pp. 210-215 (2008)
- [6.37] H. Ogura, T. Deuzé, R. Morice, P. Ridoux, J.R. Filtz, *SICE Journal of control, Measurement, and system integration*, Vol.3, No. 2, pp 81-85 (2010)
- [6.39] J.V. Pearce, C.J. Elliott, D.H. Lowe, G. Failleau, T. Deuze, F. Bourson, M. Sadli, G. Machin, Performance of Pt-C, Cr7C3-Cr3C2, Cr3C2-C, and Ru-C Fixed Points for Thermocouple Calibrations Above 1600 °C, *Int. J. Thermophys.* (to appear) (2014)
- [6.41] R.E. Bedford, *Rev. Sci. Instr.* 35, 1177 (1964)
- [6.42] T.P. Jones and K.G. Hall, The melting point of palladium and its dependence on oxygen, *Metrologia* 1979, 15, 161-163
- [6.43] P.B. Coates, T.R.D. Chandler, J.W. Andrews, A new determination of the freezing point of palladium, *High Temp – High Press.*, 1983, 15, 573-582
- [6.44] T.P. Jones, The freezing point of palladium in argon, *Metrologia*, 1988, 25, 191-192
- [6.45] F. Edler, private communication (2010)
- [6.46] T.J. Quinn and T.R.D. Chandler, The freezing point of aluminium determined by the NPL photoelectric pyrometer, *TMCSI* 4, 295-309 (1972)
- [6.47] T.J. Quinn, Corrections in optical pyrometry for the refractive index of air, *Metrologia* 10, 115 (1975)
- [6.48] T.P. Jones, J. Tapping, The freezing point of platinum, *Metrologia* 12, 19-26 (1976)
- [6.49] H. Kunz, J. Lohrengel, A new determination of the freezing point of platinum, CCT/76-10, 11th session of the CCT, Annexe T25, T197-199 (1976)
- [6.50] F. Lanza, T. Ricolfi, The IMGC determination of the freezing point of platinum, *High Temperatures - High Pressures*, 1976, volume 8, pages 217-224
- [6.51] J. Bezemer and R.T. Jongerius, *Physica*, 1976, 83c, (3), 338
- [6.52] R.E. Bedford, G. Bonnier, H. Maas, F. Pavese, Recommended values of temperature for a selected set of secondary reference points, *Metrologia* 20, 145-155 (1984)